A CAPACITIVELY COUPLED BISTABLE GAS DISCHARGE CELL FOR COMPUTER CONTROLLED DISPLAYS

Robert H. Willson

REPORT R-303 JUNE, 1966

Coordinated Science Laboratory

UNIVERSITY OF ILLINOIS - URBANA, ILLINOIS

A CAPACITIVELY COUPLED BISTABLE GAS DISCHARGE CELL FOR COMPUTER CONTROLLED DISPLAYS

Robert H. Willson

REPORT R-303 JUNE , 1966

Reprinted January, 1967

This work was supported in part by the Joint Services Electronics Program (U. S. Army, U. S. Navy, and U. S. Air Force) under Contract DA 28 043 AMC 00073(E); and in part by the Advanced Research Projects Agency through the Office of Naval Research under Contract ONR Nonr-3985-(08).

A CAPACITIVELY COUPLED BISTABLE GAS DISCHARGE CELL FOR COMPUTER CONTROLLED DISPLAYS

Robert Harry Willson, Ph.D.

Department of Electrical Engineering
University of Illinois, 1966

ABSTRACT

The capacitively coupled gas cell is made from a sandwich of three thin glass panels. A hole in the center panel forms the discharge cell and transparent electrodes on the outer surfaces of the outer panels are capacitively coupled into the cell. A simple model of the cell consisting of three capacitors and a spark gap is used to explain the bistable characteristic of the cell and the inherent electrical isolation between cells. The ratio of the firing voltage to the sustaining voltages (the voltage at which the cell refires each half cycle after the cell is first fired) has been measured for a number of cells with different gases and different pressures. In certain gas mixtures in which the discharge is very rapid this ratio has been observed to be as large as 1.8. For a cell which is .025 cm thick and .013 cm in diameter, with 300 Torr of neon and 20 Torr of nitrogen, the discharge is quenched 50×10^{-9} seconds after it is initiated and even though the duty cycle is 1/100, the average light is sufficiently intense for display purposes. In neon, the discharge develops slowly and the voltage separation is small. We suggest that photon bombardment of the negative surface controls the rapid discharge while, in the slower discharge, ion

ACKNOWLEDGMENTS

The author is deeply indebted to Professor D. L. Bitzer and Dr. H. G. Slottow for their guidance and encouragement during the course of this research and to Professor M. E. Van Valkenburg, the chairman of the final examination committee.

The author also acknowledges the importance of several conversations with Professors M. Raether, R. M. Peacock, and F. M. Propst. Discussions with Dr. F. Steinrisser and with B. W. Voth were also helpful.

Many members of C.S.L. contributed to the experiments. W. Schuemann and D. A. Lee taught the author some of their knowledge of vacuum techniques. W. P. Bleha, M. G. Craford and J. T. Jacobs taught the author some of their knowledge of thin film techniques. J. G. Burr made special tools and evaporation masks and W. J. Cummings made some of the holes in the glass by photoetching techniques. N. Vassos not only contributed to the fabrication of the experimental cell but also assisted in solving constructional problems. W. I. Lawrence did the glass work and also assisted in solving constructional problems. G. J. Crawford assisted in assembly of various cells and electronic equipment. The author would also like to acknowledge the importance of F. O. Holy, W. E. Hedges, M. A. Johnson, and W. Schmidt in building and/or maintaining various electronic equipment.

For assistance in the preparation of this report, the author is grateful to R. McFarlane, E. Conway, J. Fairchild, M. Carrera and J. Curtis.

TABLE OF CONTENTS

CHAPTER 1

INTRODUCTION

The cathode ray tube as a digital computer display is limited in several ways. First, the digital signal from the computer must be converted to an analog form and second, a memory is required from which the images can be continually regenerated. In addition, wide band transmission lines are used to connect the memory and display. In a system with only a few displays these limitations are manageable, but in the large multiple access systems now being considered they create expense and complexity. Thus, a demand exists for a simple and inexpensive display that can respond directly to digital signals and that can regenerate its own images. Arrays of gas discharge cells could, in principal, meet this demand[1], but in the past these arrays have had a number of problems which made them impractical as displays. This thesis describes a new type of gas discharge cell, which, when used as an element in a matrix display, could make the rectangular array of gas cells a practical replacement for a cathode ray tube display.

1.1 History

Under appropriate conditions a larger voltage is necessary to ignite a gas cell than is required to sustain the discharge.[2] Thus at intermediate voltages the cell is bistable, and the properties of a light source and memory are combined. Figure 1.1a shows an early design of an array of gas cells. The cells are placed between two orthogonal sets of electrodes which are deposited on the inner surface of thin

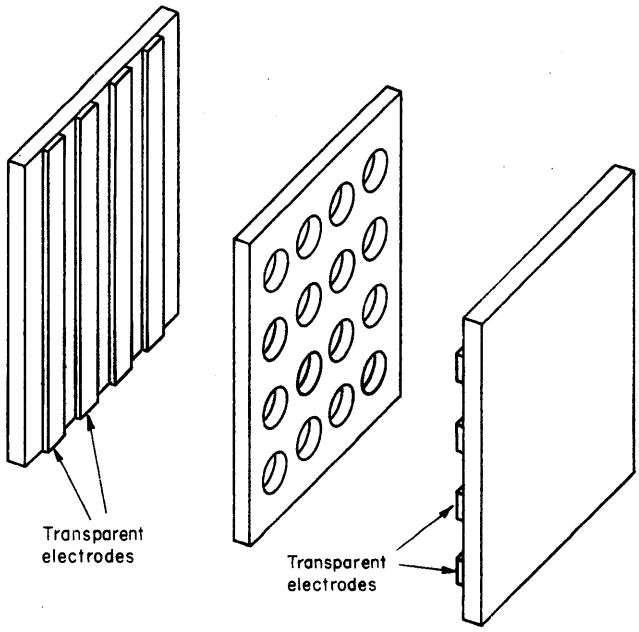

Rectangular Array of Gas Cells with Internal Electrodes

Figure 1.1a

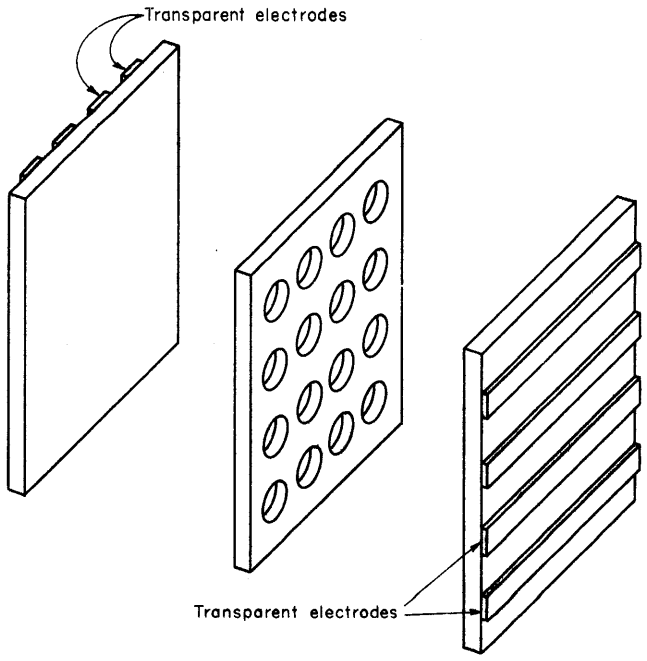

Rectangular Array of Gas Cells with External Electrodes

Figure 1.1b

flat glass plates.[3] Each electrode in the horizontal set is a common electrode for a row of cells and each electrode of the vertical set is a common electrode for a column of cells. A cell is ignited when a sufficiently high voltage is applied between the two electrodes that intersect at the selected cell. Through switching networks controlled by digital signals from a computer, any cell in the array can be selected.

One of the first rectangular arrays was made by Skellet in 1954.[4] His design had two orthogonal sets of wires which were separated by a small distance and sealed in a neon atmosphere. There were 100 horizontal and 20 vertical wires. Skellet reported that a discharge could be confined between any crossed pair of electrodes in the array. He did not report on experiments in which more than one cell was fired concurrently. However, Harris,[5] in a memorandum on the Skellet display, pointed out that when a number of cells were ignited additional unwanted cells would also fire.

Moore[3] in 1963 made a rectangular array similar to that shown in Figure 1.1a. A honeycombed glass panel was placed between the outer glass panels to isolate the cells. Transparent thin film electrodes were deposited so that the discharge could be viewed without seeing the shadow of the electrodes. The electrodes were deposited on the inside surfaces of the outer glass panels and the cells were filled with neon. Initially, Moore was interested in igniting only a single spot of light and in this he was successful. Later, when he tried to ignite a number of cells, he discovered that cells which had electrodes in common with the fired cells would also fire.[6]

Thompson,[7] in 1964, added a resistance in series with each gas cell thereby reducing the coupling between parallel electrodes. He made a small matrix of 10 x 10 cells, and demonstrated that any combination of cells could be fired without firing unwanted cells. One set of parallel electrodes was deposited as in the Moore matrix. However, the other set was isolated from the discharge cells by resistors which were connected to individual electrodes in each cell. This requires the use of one electrical feed-through connected to the face of each cell and fabrication difficulties limit both the number of cells in the display and the cell size.

1.2 New Gas Cell

In this thesis we describe a new bistable gas discharge element which has an inherent isolation impedance that should eliminate addressing ambiguities.[8,9] The physical realization is simple and the cell size can be very small. Three glass panels are laminated together. The discharge is confined to a cylindrical cavity in the center panel. The discharge is excited by signals connected to electrodes that are vapor deposited on the outer surfaces of the outer glass panels. Figure 1.2 shows an exploded view of a single cell. Since the external electrodes are capacitively coupled to the cell wall, alternating voltages are needed to excite the cell. The capacitive reactances between the electrodes and the cell walls serve as isolation impedances. Figure 1.1b shows a rectangular array made with these cells.

In certain gas mixtures, an intense cell discharge develops which deposits charge on the cell walls so rapidly that the discharge

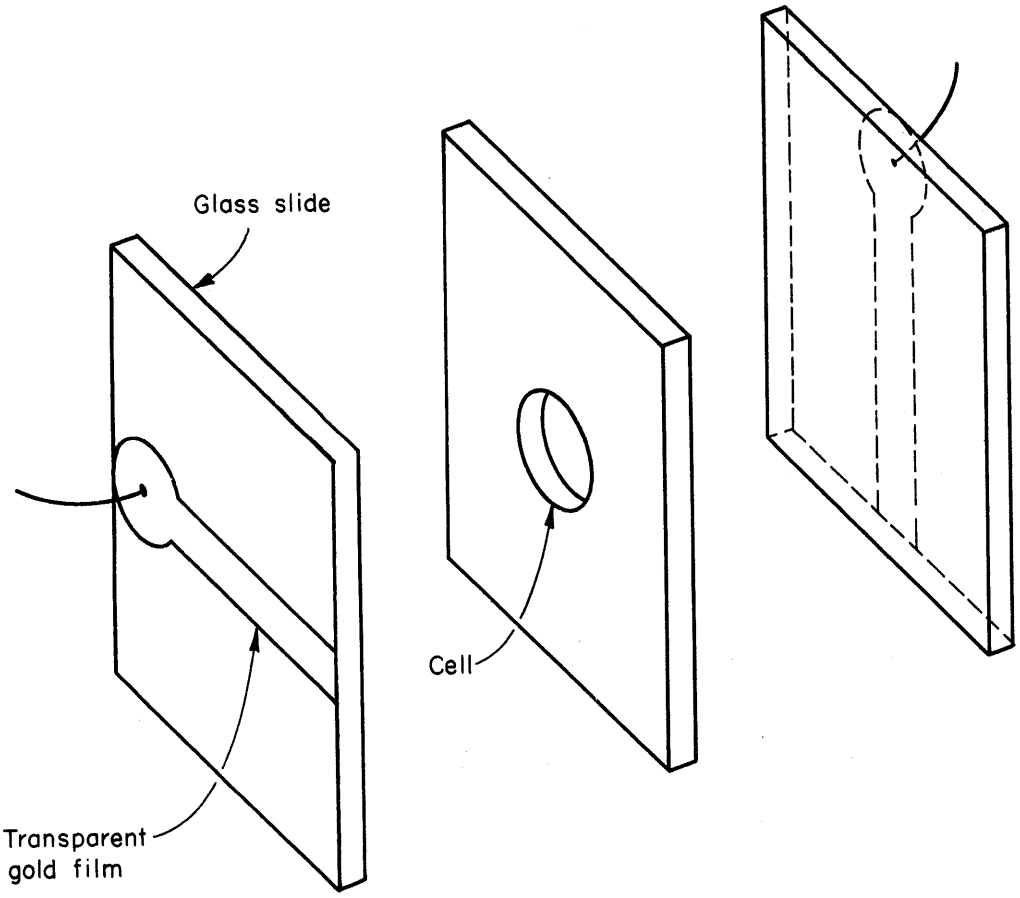

Construction of a Single Cell

Figure 1.2

is extinguished shortly after it is ignited. For instance, for the cell whose diameter is .033 cm and whose thickness is .025 cm, the discharge is extinguished only 50×10^{-9} seconds after it is ignited, yet the discharge is so intense that even with a duty cycle of 1/100 the cell is bright enough for a visual display. The presence of charges on the cell walls gives the cell its bistable characteristic. The voltage induced by the charges on the wall adds to the voltage induced by the signals on the external electrodes. Consequently, the voltage required to ignite the cell need only be the difference between the firing voltage and the wall voltage.

In Chapter 2, we discuss an equivalent circuit of this new gas discharge cell, as well as the physical processes that take place in the cell. In Chapter 3, we describe the construction details of the single cell and the experimental apparatus. In Chapter 4, we discuss the experiments that were performed on single gas cells. In Chapter 5, we discuss a switching network which could be used for coincident switching of a rectangular array of gas cells. Finally in Chapter 6 we discuss the conclusions and recommendations for further research.

CHAPTER 2

NEW BISTABLE GAS CELL WITH INHERENT ISOLATION

If, in discharges that are excited by ac signals, the charged particles were removed from the volume every half cycle, we would expect the memory mechanism to be different from that in dc discharge where the memory is space charge determined.[10] During a series of experiments to be described in Chapter 4, we discovered that in neon the discharge persisted for a relatively large fraction of the half cycle and very little voltage separation between the firing voltage and the sustaining voltage was observed. On the other hand, in neon with from 5% to 10% nitrogen, and in certain other gas mixtures, the discharge would build up rapidly, depositing charge on the cell walls in sufficient quantity to lower the voltage across the cell below the extinguishing voltage thereby turning off the discharge shortly after it was initiated. For instance, in the cell whose diameter is .033 cm and whose thickness is .025 cm, we found the discharge would be turned off 50×10^{-9} seconds after it had started, yet the radiated light was so intense under these conditions that even with a duty cycle of 1/100, the discharge provided enough light for the display. The voltage separation between the firing voltage and the sustaining voltage was large in this case, and the memory in these cells actually resides in the charges which remain on the walls from pulse to pulse. To ignite a cell with wall charges, one need only apply a voltage that may be as small as one-half the voltage needed to fire the cell in the absence of wall charges.

In this chapter, we will discuss a simple model for this new gas discharge cell. This model will be used to demonstrate the memory characteristic of the cell and the inherent series impedance which should isolate the cells when they are interconnected in an array thereby eliminating ambiguities in addressing. Finally, we will consider various physical processes that take place in the discharge cell in order to gain further insight into the operation of the cell. In particular, we will discuss the Townsend α and γ generation mechanisms, electron avalanches and rapid discharges in gases, and the source of initial electrons.

2.1 Circuit Model

Figure 2.1a shows a sectional view of the gas discharge cell and Figure 2.1b shows an equivalent circuit for the cell. Capacitor C_1 represents the capacity between an external electrode and the adjacent cell wall, capacitor C_c represents the capacity of the unfired cell, and G is a spark gap which represents the gas discharge.

Let a voltage V_d' be applied between terminals a and b. The voltage across the cell, V_c, will have two components, V_d which is proportional to the external voltage V_d', and V_o which is proportional to the charge Q on the cell walls:

$$V_c = V_d + V_o \tag{2.1}$$

where

$$V_d = \left(\frac{C_1}{C_1+2C_c}\right)V_d' \tag{2.2}$$

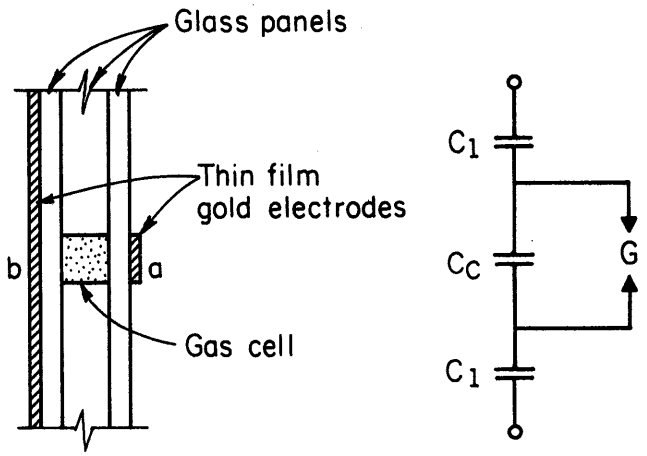

Sectional View and Equivalent Circuit

Figure 2.1

and

$$V_o = \frac{Q}{C_c} \quad . \tag{2.3}$$

When a discharge occurs, charge flows to the walls leaving them charged to a voltage V_o. Between discharges, the walls remain charged to V_o, since the charge leakage time is orders of magnitude longer than the time between firings. A discharge occurs when a sufficiently large voltage, called the firing voltage, V_f, appears across the cell. The firing voltage as applied across terminals a and b is V_f'. If the walls are uncharged, the external signal, V_d', must supply the entire firing voltage. That is, using Equations 2.1 and 2.2 we have

$$V_d' \geq \left(\frac{C_1+2C_c}{C_c}\right)V_f \quad . \tag{2.4}$$

However, if the wall is charged, V_o is not equal to zero and V_d need only be as large as $V_f - V_o$ to fire the cell. Calling this voltage the sustaining voltage, V_s', we have

$$V_s' = \left(\frac{C_1+2C_c}{C_c}\right)(V_f - V_o) \quad . \tag{2.5}$$

At any voltage between V_f' and V_s' the cell has a bistable characteristic, and the state of the cell is determined by the presence or absence of the wall voltage, V_o.

A convenient figure of merit, M, which indicates how completely the cell walls have been charged, is defined as follows:

$$M = \frac{V_f'-V_s'}{V_s'} \times 100\% \tag{2.6}$$

If the walls are not charged, V_f' is equal to V_s', and M = 0%. If on the other hand the wall charges completely, neutralizing the field inside the cell, then $V_f' = 2V_s'$ and M = 100%.

Consider the cell with a sinusoidal voltage V_d across it as shown in Figure 2.2, and assume that the cell fires at symmetrical points every half cycle. These points are marked in the diagram by horizontal lines and occur at times t_1 and t_2. At time t_1, just before the cell fires, V_d is equal to $V_1/2$, and the total voltage across the cell, V_c, is V_f so

$$V_c = V_f = V_o + \frac{V_1}{2} \tag{2.7}$$

Just after the discharge, the total voltage across the cell is given by

$$V_c = V_f - \Delta V \tag{2.8}$$

where ΔV is the voltage change across the cell caused by the flow of charge to the cell walls. Voltage V_d does not change appreciably during the brief discharge time. At time t_2 the voltage across the cell is $-V_f$ and since V_d has changed by $-V_1$ volts from the value it had at time t_1, we have that

$$V_c = -V_f = V_f - \Delta V - V_1 \tag{2.9}$$

and combining Equations 2.7 and 2.9, we obtain that

$$\Delta V = 2V_o \ . \tag{2.10}$$

The total voltage change across the cell caused by charge transfer, ΔV, is less than or equal to V_f. In the steady state, Equation 2.10

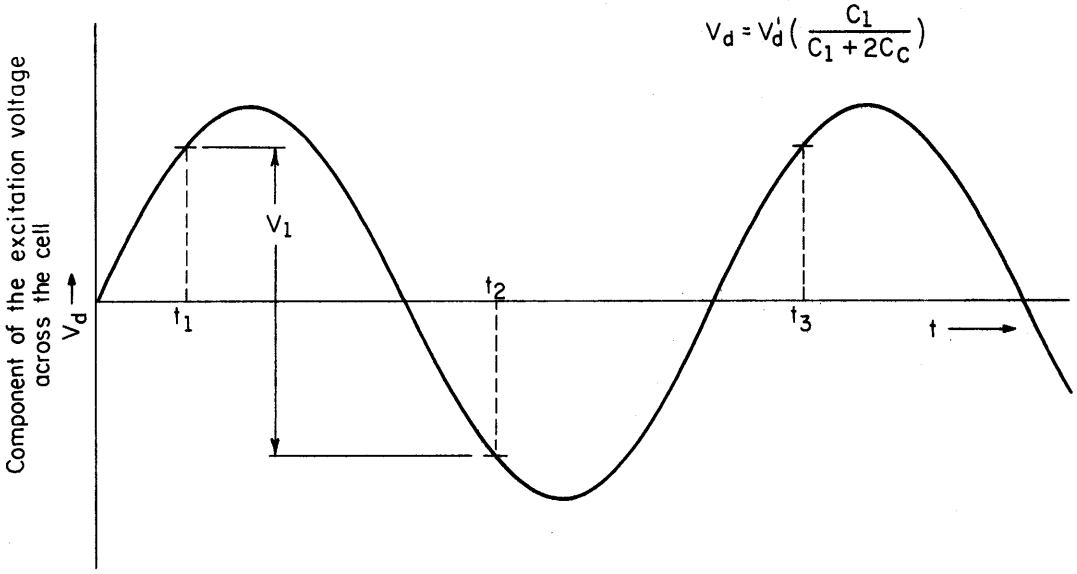

Sine Wave Voltage

Figure 2.2

holds, and we have that

$$V_o \leq \frac{V_f}{2} . \tag{2.11}$$

We would expect from our model that with sufficiently high voltages the cell should fire twice each half cycle, and experiments discussed in Chapter 4 show that this is indeed so. We can derive a useful equation for V_f and V_o in terms of the applied voltages for the case in which the cell fires twice each half cycle as follows: Figure 2.3 shows a voltage waveform which fires the cell at times t_1, t_2, t_3 etc. Using Equations 2.8 and 2.10, the total voltage across the cell at time t_1 just after the discharge is

$$V_c = V_f - 2V_o \tag{2.12}$$

At time t_2, the voltage V_d has increased by V_3 volts and the cell voltage, V_c, is equal to V_f firing the cell. On the other hand, it is clear from Equation 2.12 that by adding a voltage $2V_o$ to the cell voltage, that the cell will fire again. Thus $2V_o$ is equal to V_1 and

$$V_o = \frac{V_1}{2} . \tag{2.13}$$

After the discharge, the cell voltage has decreased by $2V_o$ volts. The voltage V_d continues to rise but not enough to fire the cell, however during its negative excursion at time t_3, V_d has decreased by $-V_2$ volts and it reaches a level such that the cell voltage is equal to $-V_f$ and the cell fires a third time. Thus

$$V_c = -V_f = V_f - 2V_o - V_2 \tag{2.14}$$

and combining Equations 2.13 and 2.14 we obtain the following expression

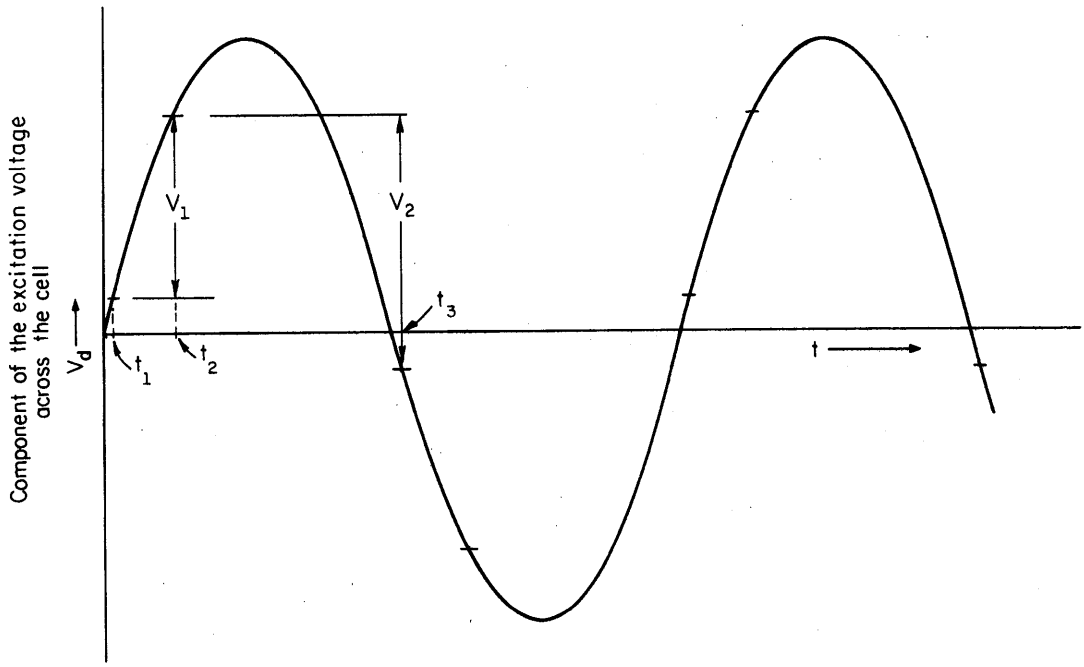

Large Sine Wave Voltage

Figure 2.3

for the firing voltage

$$V_f = \frac{V_1+V_2}{2} \quad . \tag{2.15}$$

Although voltages V_f, V_1 and V_2 are all internal voltages which are measured directly across capacitor C_c, they are proportional to voltages V_f', V_1', and V_2', respectively, measured across terminals a and b. The proportionality factor is given by Equation 2.2 and is $C_1/(C_1+2C_c)$. Equations 2.13 and 2.15 provide another method for determining V_o and V_f.

Experimental data in Chapter 4 shows that the cell does indeed fire twice each half cycle. If V_d is raised further, the cell should fire three times each half cycle, then four times, etc. We have observed the three firings each half cycle.

In the above we have assumed that the discharge develops rapidly and is turned off in a very short time. Whether this is so, or not, depends on the gas mixture. For instance, in neon or argon, the discharge is slow in developing and in turning off and the model is not applicable. But in neon plus 10% of a molecular gas, or in nitrogen, the discharge develops rapidly and sufficient charge flows to reduce the cell voltage below the sustaining voltage and the discharge is extinguished shortly after it was started. In this case the above model is applicable.

We asserted in Chapter 1 that unwanted cells would fire in arrays made of dc discharge cells, while arrays made with the present cells would be free from this problem. Let us now consider why this

is so. A current limiting impedance must be used with a dc gas discharge cell to limit the cell current, and typically this impedance is one hundred thousand ohms.[2] In Figure 2.4 a simple 2 X 2 matrix is shown and in each horizontal and vertical line there is a voltage source, V'/2 and the current limiting impedance Z_s. These voltages add across adjacent cells so that a sustaining voltage is applied to each cell. We have assumed that cells b and d are on, and we wish to fire cell a. Sufficiently large voltage sources, $V_g'/2$, are added to row 1 and to column 1 to fire cell a. If cells b and d were not on, only cell a would fire. With these cells on, however, rows 1 and 2 are coupled together through the low impedance of cells b and d. Since these cell impedances are much smaller than impedance Z_s, the voltage on rows 1 and 2 would be practically the same and both cell a and c would be fired. As we pointed out in Chapter 1, Thompson[7] alleviated this problem by adding a series resistor to each of the cells. With this procedure, however, fabrication is difficult and the attainable cell density would seem to be severely limited. On the other hand an array of capacitively coupled cells seems to be immune from this problem. The capacitive reactance between the external conductors and the gas cells are each of the order of 10^7 ohms (at 10^5Hz). Therefore the source impedances can be as large as 10^5 ohms and each cell is still isolated from its neighbor.

2.2 Gas Breakdown

In order to understand the physical processes that give the cell its characteristics, we will now consider that part of Physics

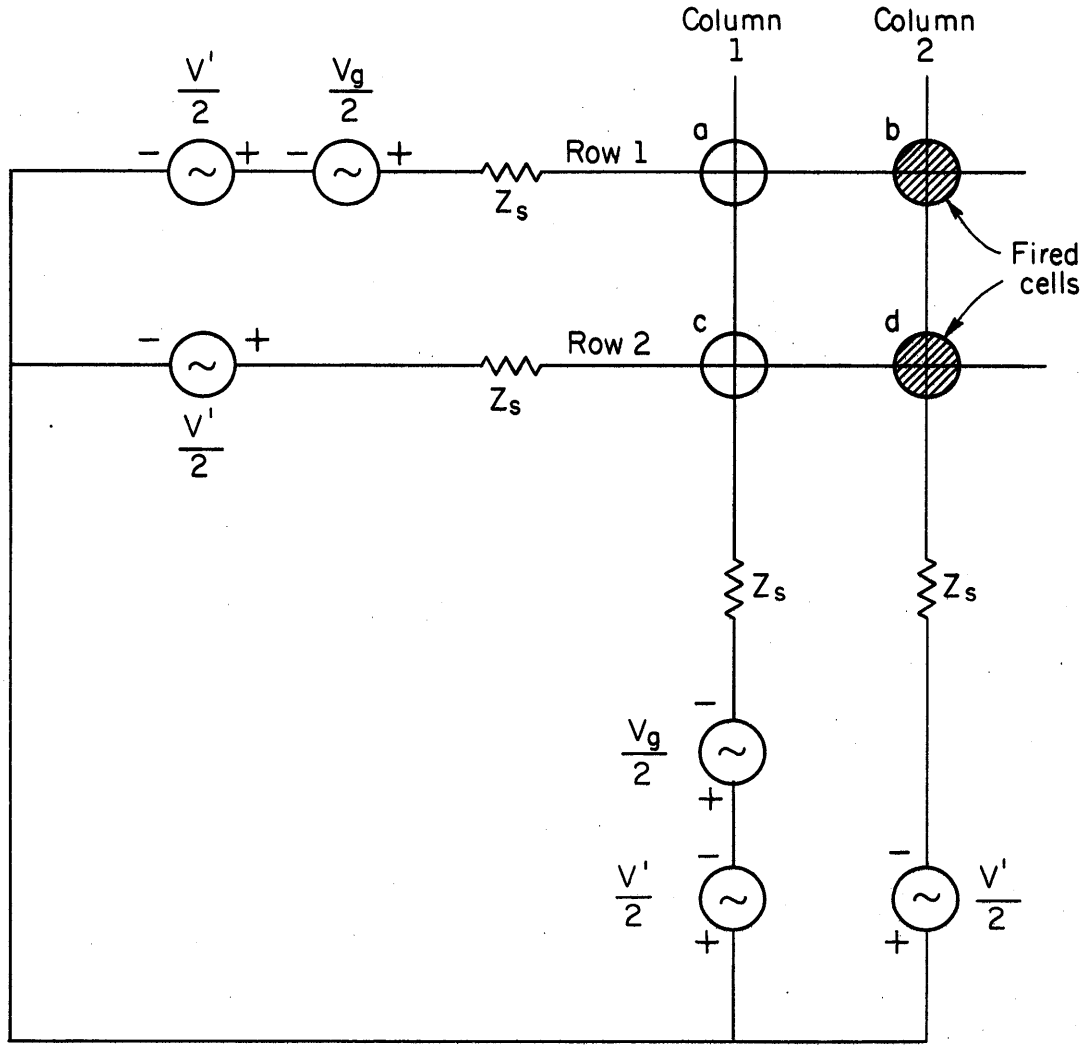

Simple 2 × 2 Array

Figure 2.4

which applies to gas discharges in the capacitively coupled cell. First, we will discuss the electron multiplication mechanisms and electron avalanches and show that in pure neon at 40 Torr that a relatively slow mechanism, positive ion bombardment of the negative surface, determines breakdown, but that in nitrogen a much faster secondary mechanism, photon bombardment of the negative surface, determines breakdown. Finally, we suggest that the electrons required for the initiation of each discharge are produced by collisions of metastable atoms with the walls of the cell.

For a discharge to occur in a gas, the primary electrons must create large numbers of secondary electrons. This process of electron multiplication is described by the Townsend α coefficient. On the average, each primary electron with sufficient energy creates α electron ion pairs per cm of path traveled in the field direction. The Townsend coefficient, α, divided by the pressure, p, is a function of the ratio of the electric field to the pressure (E/p), and for a given pressure and cell thickness, d, α is determined by the cell voltage, V. If there are n_o initial electrons and the distance required for an electron to gain its equilibrium energy is d_o, then the n_o electrons create $n - n_o$ additional electrons in moving a distance d. The total number of electrons, n, is given by

$$n = n_o \exp(\alpha(d-d_o)) \tag{2.16}$$

In Equation 2.16, we have assumed that the field is small and uniform across the discharge gap. At higher values of the electric field, secondary multiplication mechanisms become important, and the number

of electrons grows larger than that predicted by Equation 2.16. This increase can be accounted for by two secondary mechanisms, β mechanisms, which take place in the gas, and γ mechanisms which take place at the cathode. The most important β mechanisms are:

1) photoelectric effect in the gas which is described by β_p which expresses the number of electron-ion pairs created per cm per photon,
2) ionization by collisions of the second kind, i.e., the Penning effect in which excited atoms or molecules in the gas ionize other atoms of the gas.[11,12,13]

The most important γ mechanisms are:

1) positive ion bombardment of the cathode which is expressed by γ_i, the number of electrons per incident ion, where γ_i is a function of E/p,
2) the photoelectric effect at the cathode designated by γ_p, the number of electrons per photon, where γ_p is a function of wavelength, λ,
3) excited atoms, especially metastable states, hitting the cathode, where this process is designated by γ_m, the number of electrons per incident excited atom.[11,12,13]

Brown[14] points out that as E/p decreases there is a transition of the secondary mechanism from γ_i to γ_p to β_p. The term β_p is only important in extremely rapid discharges and, as we shall see, in discharges which are more rapid than those which we investigated.

In gases which have large ionization potentials, γ_i is the dominant secondary process, and the presence of surface films significantly reduces γ_i.[12] On the other hand, γ_p is dominant in a gas which has a large ratio of the number of exciting collisions to the number of ionization collisions and the presence of surface films enhances γ_p.[12] Molecular gases readily adsorb on surfaces while inert gases do not[15] so normally, these factors make γ_i the most important secondary mechanism in neon discharges, and γ_p the most significant secondary mechanism in nitrogen discharges. Although γ_m is only important as a secondary mechanism in discharges that develop much slower than the discharges studied here, we shall see that γ_m is important in the discharges studied because γ_m can produce initial electrons for succeeding discharges.

Loeb[13] points out that all of these secondary mechanisms, except collisions of the second kind, lead to the same form of current equation, which in terms of an initial current i_o is

$$i = \frac{i_o \exp(\alpha(d-d_o))}{1-\gamma(\exp(\alpha(d-d_o))-1)} . \qquad (2.17)$$

Francis[12] adds that if a number of independent γ mechanisms are operative at the same time then

$$\gamma = \gamma_i + \gamma_m + \bar{\gamma}_p \qquad (2.18)$$

where $\bar{\gamma}_p$ is the effective value of the secondary emission coefficient due to photon bombardment and expresses the number of electrons emitted from the negative surface divided by the number of ions created in the volume and is equal to $f \cdot Z \cdot \gamma_p$. The ratio of the number of photons that

strike the cathode to the total number of photons created in the volume is given by the factor f, the ratio of the total number of photons to the number of ions produced in the gas is given by Z, and the photoelectric yield is given by γ_p. An equation of exactly the same form as Equation 2.17 is obtained when β_p is the dominant secondary process.[12]

If in Equation 2.17,

$$\mu = \gamma(\exp(\alpha(d-d_o))-1) = 1 \qquad (2.19)$$

the current is undefined. However, this condition predicts the voltage at which the current becomes self sustaining in the sense that it is independent of external sources, i_o.[12,13] This voltage is called the ignition or firing voltage. Table 2.1 lists the value of the ignition voltage, V_f, for neon and nitrogen which were given by Penning[16] for a dc discharge between parallel plates together with the firing voltage which we measured for these gases in the experimental cell. We see that the ignition voltage of the cell is approximately the same as that of a dc cell (of the same thickness and pressure). Equation 2.2 has been used to convert the firing voltage, V_f', as measured across terminals a and b to the cell firing voltage, V_f. Setting $\mu = 1$, we have that in pure neon $\gamma_i = .023$. The value of α for this calculation is listed in Table 2.2, p. 26. This value is reasonable for positive ion bombardment of metal surfaces for an E/p equal to 62, the value of E/p in the experimental cell, and it is believed that glass surfaces would have similar γ_i's as those found in metals.[11] On the other hand, setting $\mu = 1$ in nitrogen gives that $\bar{\gamma}_p = 6.0 \times 10^{-4}$. Following Francis,[12] we let f equal the solid angle subtended by the cathode at

Gas	V_f volts (a)	V_f (zero to peak) volts (b)
Ne	250	248 ± 20
N_2	700	681 ± 50

(a) Penning, "Mechanism of Electrical Discharges in Gases of Low Pressure," Rev. Mod. Phys., V12, No. 2, p. 114 (1940).

(b) Measured

Comparison of V_f Measured and V_f from the Literature

Table 2.1

the middle of the anode divided by 4Π and we have that $f \approx .1$. Loeb[13] gives that the ratio of excited states to ionized states in nitrogen, for an E/p equal to 170, is 3.33 and using Loeb's number as the number of photons per ion, we have that $\gamma_p = 1.8 \times 10^{-3}$. Coefficient γ_p is a function of wavelength and von Engel[11] gives that for soft glass, at $\lambda = 2537\text{Å}$, $\gamma_p \approx 6 \times 10^{-4}$ while at wavelengths much shorter than 1250Å, $\gamma_p = 10^{-2}$. The strongest line in the nitrogen spectrum is at 1135Å,[17] and is probably the major contributor to γ_p. Thus we see that the calculated γ_p is consistent with the von Engel data.

The electrons and ions that a single electron generates in going from the cathode to the anode forms an electron avalanche. The secondary electrons are released from the cathode by the γ process T seconds after the initial electron is released from the cathode, and time T is called the avalanche time. Each avalanche creates $\gamma(\exp(\alpha(d-d_o))-1)$ new electrons and we see that Equation 2.19 expresses the limiting condition for charge to accumulate in the volume from successive avalanches. If γ_p is the principal secondary mechanism, the secondary electrons appear in about one electron transit time T_- which is equal to d/v_- where v_- is the electron velocity while if γ_i is the principal secondary mechanism, the electrons appear in about the ion transit time T_+ which is equal to d/v_+ where v_+ is the ion velocity. Knowing the avalanche transit time enables one to separate these two mechanisms.[18]

During the current buildup, a nearly constant voltage is applied since the time required for breakdown is short compared to a quarter cycle of the applied voltage, and we would expect that the buildup of current which ultimately leads to a breakdown in the experimental cell is the same as that in a dc cell. The high dielectric constant of the soft glass, $\epsilon = 7.2\epsilon_o$, makes the coupling capacity, C_l, much greater than the cell capacity, C_c, and using Equation 2.2 we have that, depending on cell size, approximately 85% to 95% of the external voltage will be applied across the inside surface of the cell. Of course once breakdown has occurred the characteristics of the cell are completely different from those of a dc discharge cell.

Although a complete quantitative explanation of the breakdown mechanism for different gas mixtures is not yet known, a qualitative explanation is known, and a few quantitative calculations can be made. Two different types of discharge are known and in both, a large space charge is formed. However, the manner in which the space charge builds up is different in the two cases. In the first case, the space charge is due to the relatively slow positive ions which are left from succeeding electron avalanches. Discharges of this type are called generation or Townsend discharges, and the time required for breakdown to occur is long compared to the development time of the individual electron avalanches. In the second case, the space charge is built up in less than one electron avalanche time, and indeed it is the space charge which acts directly on the electron

avalanche to build the complete discharge. This type of discharge is called a streamer.[13,18,19]

In a streamer an electron avalanche generates approximately $n_o \exp(\alpha d)$ electron ion pairs in a distance d. Empirical results from cloud chamber experiments,[18] show that the number of charges in a streamer is of the order of 10^8 electron ion pairs. Thus if the avalanche develops from a single electron, then we have that $\alpha d \approx 20$. Since the streamer develops in approximately the time required for an electron to move the distance d we find that the streamer breakdown time, T_{br}, is[18]

$$T_{br} \approx \frac{d}{v_-} \approx \frac{20}{\alpha v_-} . \qquad (2.20)$$

With the generation mechanism, however, breakdown only occurs after a number of avalanches have developed and the time for each avalanche is either T_+ or T_- seconds depending on whether the secondary mechanism is γ_i or γ_p.

In Table 2.2 the measured breakdown time, T_m, the avalanche times T_- and T_+, and the streamer breakdown time, T_{br} given by Equation 2.20 are listed for neon and nitrogen. In both cases we see that the streamer breakdown time is less than the measured breakdown time. This suggests that the generation mechanism rather than the single streamer leads to breakdown.

Once current starts to flow, charge is deposited on the cell walls. If the formative time of the current is short compared to the time variation of the applied voltage, the charge reduces the

Gas	E/p $\frac{\text{volts}}{\text{cm} \times \text{Torr}}$	V_f volts (a)	α $\frac{\text{ions}}{\text{cm}}$	τ_m seconds (a)	M (b)	v_- $\frac{\text{cm}}{\text{sec}}$	v_+ $\frac{\text{cm}}{\text{sec}}$	$T_{Br} = \frac{20}{\alpha v_-}$ sec	$T_+ = d/v_+$ sec	$T_- = d/v_-$ sec
Ne	62	240	42 (e)	2.3×10^{-6}	8	4×10^{7} (c)	1.2×10^{5} (d)	11.9×10^{-9}	834×10^{-9}	
N_2	170	681	76 (e)	20×10^{-9}	76	5×10^{7} (c)	2.5×10^{5} (c)	5.4×10^{-9}		2×10^{-9}

(a) Measured data for the cell .133 cm in diameter and .1 cm thick

(b) $M = \frac{V_f' - V_e'}{V_e'} \times 100$

(c) Raether, Electron Avalanches and Breakdown in Gases, Butterworth, Inc., Washington, D.C., 1964

(d) Loeb, Basic Processes of Gaseous Electronics, University of California Press, Berkeley, 1961

(e) von Engel, Ionized Gases, Clarendon Press, Oxford, 1966

Useful Data

Table 2.2

voltage across the cell below the extinguishing voltage thereby quenching the discharge. If the total cell voltage, V_c, does not change sign, the remaining charge in the volume continues to flow to the walls, reducing the cell voltage still further. If there is still charge in the volume when the cell voltage, V_c, changes sign the charge flow reverses. This reduces the cell voltage, V_o, below what it otherwise would be, but more important, it partially counteracts the earlier charging of the cell walls. Thus discharges which take longer times to develop will create smaller wall voltages, V_o, and consequently smaller figures of merit than discharges which are faster. This type of phenomena is characteristic of the discharge in nitrogen and in neon plus nitrogen. In neon alone, however, the discharge develops sufficiently slow so that the above analysis is not applicable.

To provide the electrons required to initiate the first discharge, we illuminate the cell with light from an ultraviolet lamp. However, for succeeding discharges we find that these photo-electrons are not necessary. This suggests that electrons are produced by some mechanism associated with the previous discharge.

The discharge creates electrons, ions, photons and both normal and metastable excited states. Except for the metastable states, these particles, for the most part, are destroyed or leave the volume in the time interval between discharges. The metastable states are neutral and diffuse to the walls unless they are destroyed by collisions in the volume. Nitrogen metastables are buffered by

neon and nitrogen[13] and when they collide with the wall there is a high probability that an electron will be ejected into the gas.[12]

The diffusion time constant in a cylindrical cell of radius r and height d is[14]

$$\tau = \frac{1}{D}\frac{\Pi^2}{d^2} + \frac{2.405}{r^2} \qquad (2.21)$$

where D is the diffusion coefficient. In the two cells on which most measurements were made, the calculated values of τ were 43×10^{-6} seconds and 100×10^{-6} seconds, and we see that both are long compared to the time between firings. We have observed, however, that with the voltage waveform shown in Figure 3.4c, p. 36 when the time between firings is extended beyond 100×10^{-6} seconds, the cell fails to ignite.

CHAPTER 3

CONSTRUCTION OF A SINGLE CELL AND EXPERIMENTAL SET UP

In this chapter we discuss the construction details of a single cell and the experimental procedure used to measure the excitation voltage, discharge current, and light output for the single cell.

3.1 Construction of the Cell

The cell is constructed from three pieces of flat glass sandwiched together. A small hole is drilled through the center piece, and transparent electrodes are deposited on the outside surfaces of the outer glass panels. Figure 3.1a shows an exploded view of the cell. The outer pieces of flat glass are .015 cm thick and the inner piece is typically .100 cm thick although .050 cm thick and .025 cm thick pieces were sometimes used. A number of different size holes were made ranging from .152 cm to .028 cm in diameter.

The electrodes consisted of evaporated gold film 100 Å thick. The width of each electrode is approximately equal to the diameter of the hole. Small wires are attached to the gold with indium solder, and the exterior surfaces of the flat glass are sprayed with a clear plastic to protect the gold. The glass assembly is bonded with epoxy to a pyrex glass pull-off tube as shown in Figure 3.1b.

3.2 Vacuum System

The vacuum and gas filling system is shown in Figure 3.2. The vacuum pumping system consists of a standard oil diffusion pump

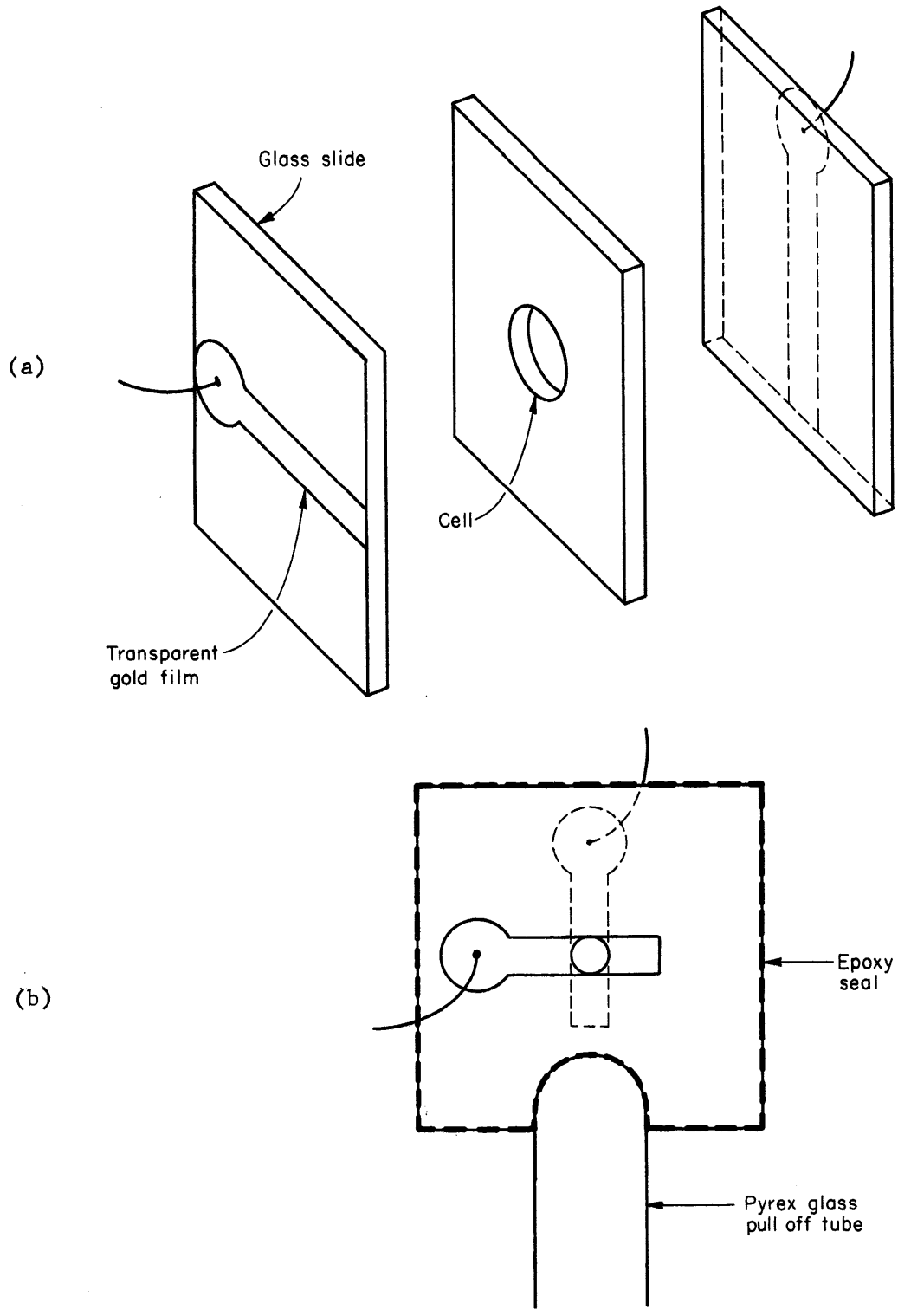

Exploded View and Construction of a Single Cell

Figure 3.1

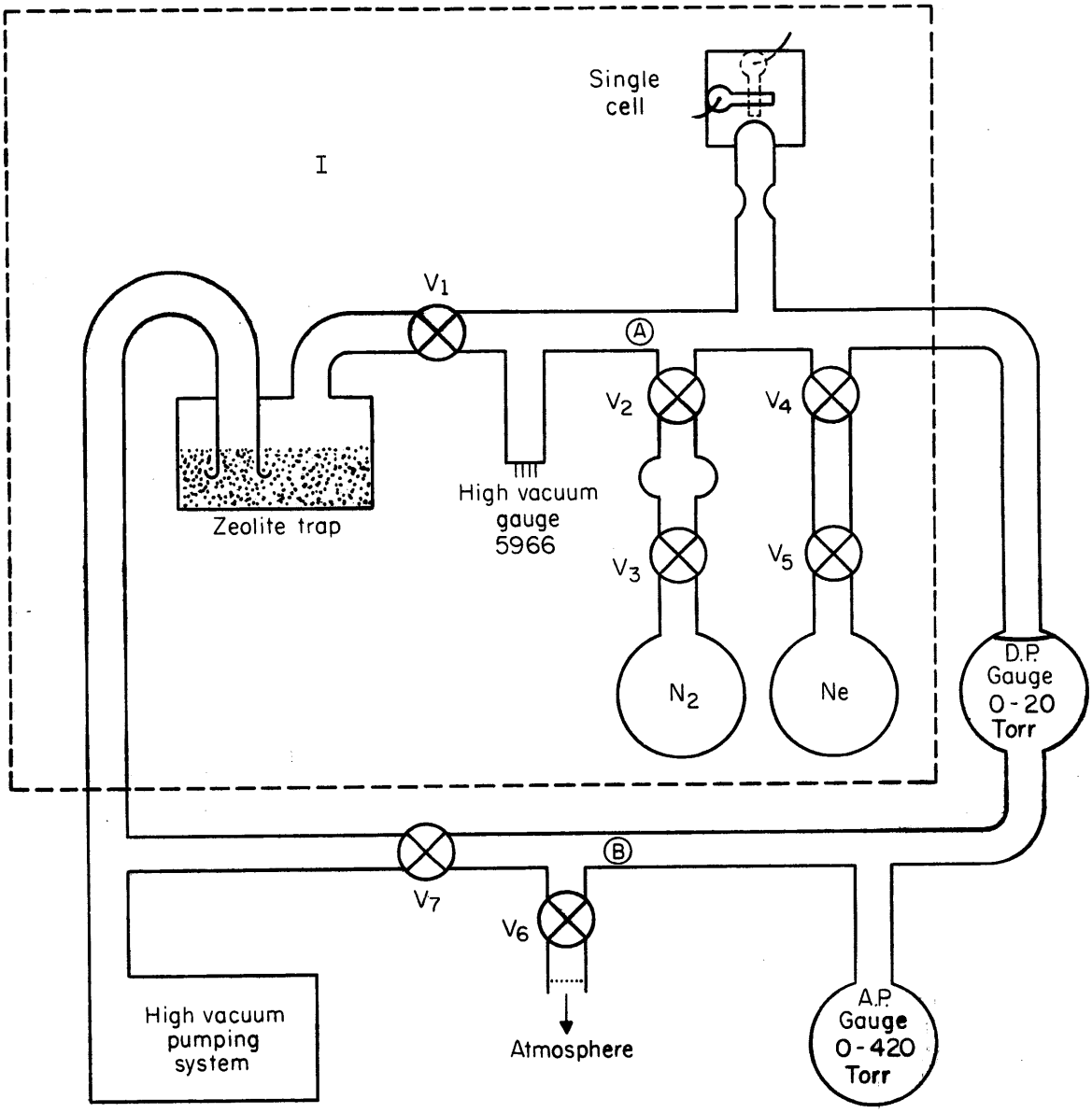

Vacuum and Gas Filling System

Figure 3.2

and fore pump.[15] Bakeable high vacuum valves are used and double valves V_2, V_3 and V_4, V_5 are used to reduce back streaming of gas into the gas bottles. The part of the system within the dashed rectangle in Figure 3.2 can be baked at 150° C. To attain pressures in the 10^{-6} Torr range, it is sufficient to bake only the zeolite trap at 300° C.

To avoid the need for low temperature traps Wallace-Tiernan mechanical monometers are used instead of mercury or oil monometers. One gauge (A.P.) is an absolute pressure gauge with a full scale deflection of 420 Torr, a sensitivity of .8 Torr, and an accuracy of $\pm$1.14 Torr. The vacuum side of the bellows in this gauge is permanently sealed off and the case side is connected to volume B. A second gauge (D.P.) is a differential pressure gauge with a full scale deflection of 20 Torr, a sensitivity of .04 Torr and an accuracy of $\pm$.06 Torr. The vacuum side of the bellows of this gauge is connected to volume A and the case side is connected to volume B. This two gauge arrangement is used both to reduce the contaminants in volume A and to reduce the volume of volume A. The normal procedure is to add neon to volume A and balance this pressure by letting air into volume B through valve V_6. The absolute pressure gauge indicates the pressure of neon in volume A. Small amounts of nitrogen can then be added to volume A and the small nitrogen pressure is indicated on the differential pressure gauge. For the cell with a diameter of .133 cm and a thickness of .1 cm, typical partial pressures were 40 Torr of neon and 4 Torr of nitrogen. Because of an extremely small conductance

between the cell and the rest of volume A, ten minutes were allowed for gas to diffuse into the cell before data is taken.

3.3 Experimental Set Up

In every case, the current, voltage, and light output signals were displayed on a Tektronix #585 oscilloscope. The experimental set up is shown in Figure 3.3. The current flowing in the cell was determined from the voltage across a resistor in series with the cell. This resistor was sufficiently small so that the bandwidth was only limited by the oscilloscope and its preamplifier. Resistor R was usually equal to 100Ω and the rise time was of the order of 2×10^{-9} seconds. The voltage across the cell was not significantly affected by R because R was very much smaller than the capacitive reactance of the cell. The preamplifier used in measuring the fastest waveforms had a rise time that was less than 2.5×10^{-9} seconds. A 100x passive probe was connected directly across the cell and resistor R to measure the cell voltage.

The light from the cell is channeled through a fiber bundle "light pipe" onto the cathode of a photomultiplier. The coaxial cable between the photomultiplier anode and the linear amplifier is terminated at both ends by 100Ω. This amplifier had a bandwidth of 17×10^{6} Hz, so the fastest rise time that could be observed was 20×10^{-9} seconds.

The cell is usually excited by a sine wave whose amplitude can be varied from 0 to 1000 volts rms and whose frequency can be varied from 50 KHz to 40 KHz. This voltage can be pulsed on and off

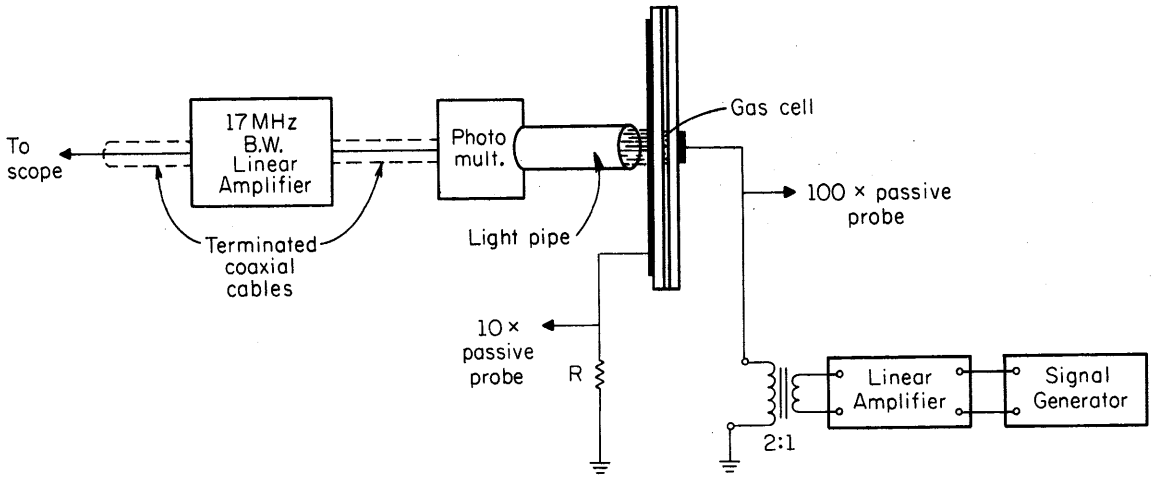

Experimental Set Up

Figure 3.3

for controlled intervals of time. A wavetrain of this signal is shown in Figure 3.4b. The on time, T_1, was normally 3×10^{-3} seconds and the off time, T_2, was 33×10^{-3} seconds. Another generator provided the pulse signals as shown in Figure 3.4c. Each pulse waveform was a full cycle of a sine wave.

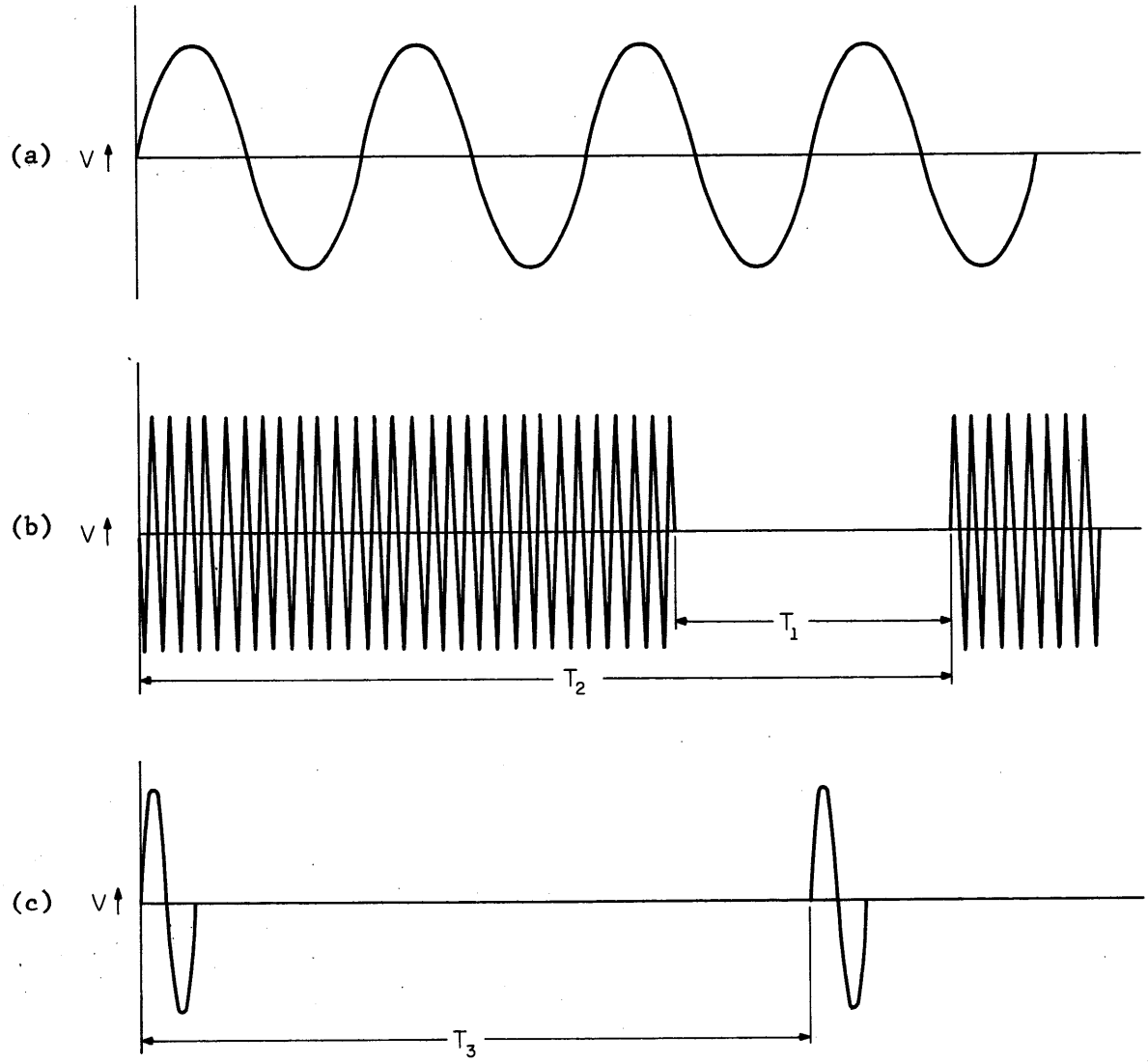

Different Excitation Voltages

Figure 3.4

CHAPTER 4

EXPERIMENTAL RESULTS

Measurements of the current and the radiated light in the capacitively coupled discharge cell show that the behavior with neon contrasts markedly with the behavior with some gas mixtures and with some molecular gases. Discharges in neon or argon are generally characterized by long pulses and small figures of merit (little memory) whereas discharges in neon plus a molecular gas are characterized by sharp pulses and large figures of merit. In this chapter we describe these measurements in detail.

4.1 Measurements of Pulse Shapes in Rare Gas Discharges

All of the experiments which are described in this section were performed on a cell .1 cm thick and .133 cm in diameter. The frequency of the sinusoidal excitation voltage was 100 KHz. In Figure 4.1a is shown an oscillogram of the light output and excitation voltage for the neon discharge at 40 Torr. The light is seen to be modulated at the second harmonic frequency of the excitation signal. To establish a dark level, the signal was interrupted once every 33×10^{-3} seconds and the off time was varied from 10^{-5} seconds to 2×10^{-2} seconds. The dark level coincided with the minimum of the light trace shown in Figure 4.1a. From this and from the shape of the curve we conclude that the discharge persists for a large fraction of a half cycle.

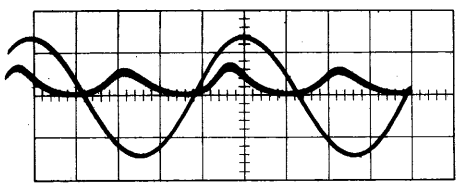

(a)

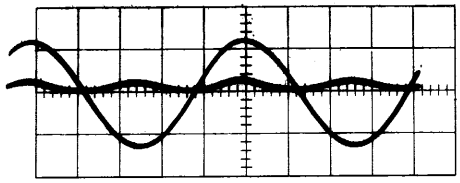

(b)

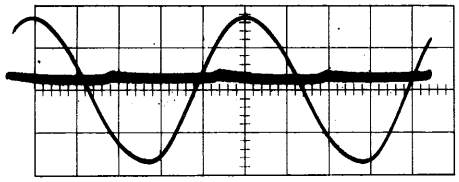

(c)

2μs/div

Light Pulse and Voltage Pulse

Figure 4.1

As the pressure of neon is raised to 140 Torr, the only change in the light pulse is a moderate decrease in light output. An oscillograph of the light and excitation voltage is shown in Figure 4.1b.

With argon at a pressure of 40 Torr, the discharge was extremely dim and could barely be seen on the oscillograph. A comparison of the argon light pulse shown in Figure 4.1c with the neon light pulse in Figure 4.1a shows that the argon pulse is somewhat narrower.

4.2 Influence of Cell Geometry on the Neon Discharge

To study the effect of cell geometry eight different cells were constructed and we list the dimensions of these cells in Table 4.1. The firing voltage, V_f', and the sustaining voltage, V_s', (which is equal to $V_f' - V_o'$ where V_o' is the wall voltage times $(C_l + 2C_c)/C_c$ are nearly equal in neon because the discharge does not build up an appreciable wall voltage. We observed little change in the cell characteristics as the frequency was varied from 60 KHz to 300 KHz. In Figure 4.2 we show the sustaining voltage as a function of pressure for the different cells. We see that for each cell there is a pressure for which this voltage is a minimum. The actual value of this minimum varies from cell to cell. If we restrict our attention to those cells for which d is constant, for example cells "c," "f" and "i" all have d = .025 cm, this minimum voltage changes with r and in fact there seems to be a minimum of the minima. In the example cell "f" has the minimum of the minima.

Cell	d cm	r cm
"a"	.10	.066
"b"	.05	.061
"c"	.025	.076
"d"	.10	.050
"f"	.025	.047
"g"	.10	.018
"h"	.05	.014
"i"	.025	.017

Cell Thickness d and Radius r for the Various Cells

Table 4.1

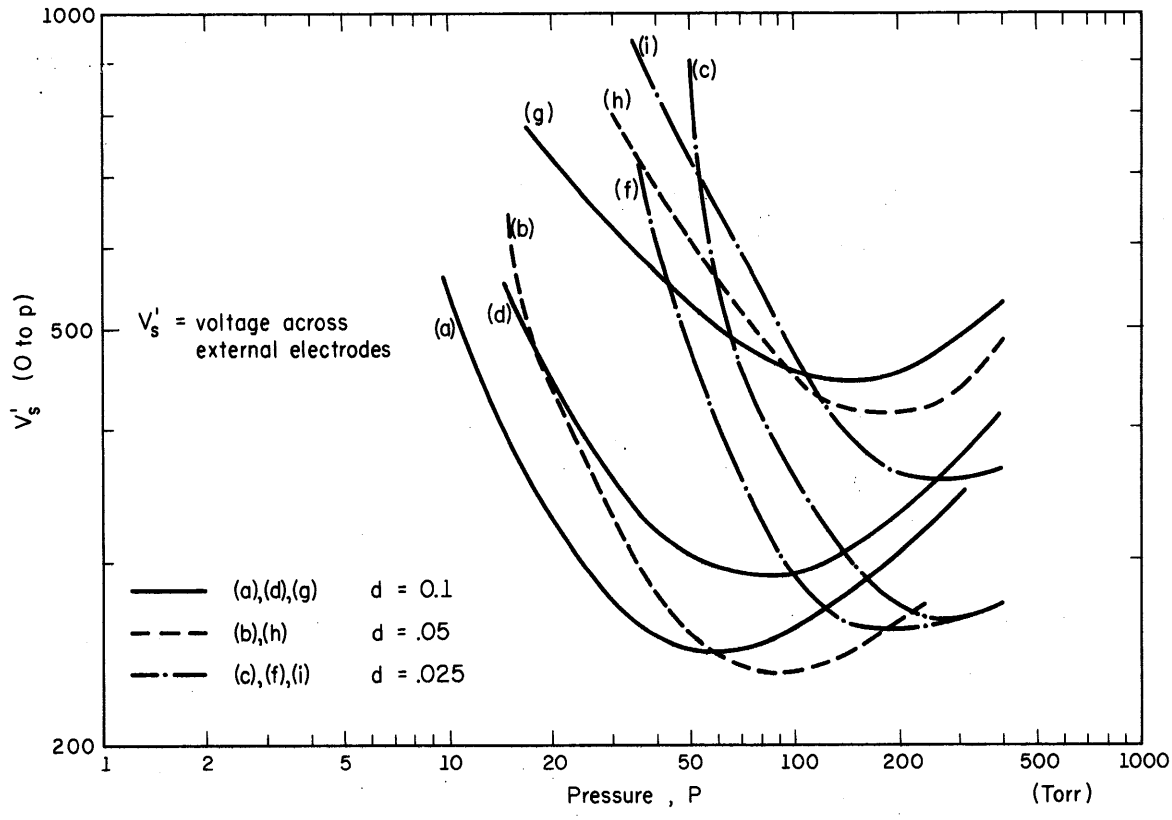

Sustaining Voltage vs. Pressure

Figure 4.2

This seems to be true for other values of d as well. It would be interesting to learn whether this minimum is a function of r and d independently or a function of r/d but more data will have to be taken to be able to say more about this optimum. Table 4.2 lists the various r/d ratios arranged in order of the voltage minimum and the cell thickness. The frequency of the sustaining voltage was 100 KHz.

Cells "a" and "i" have the same r/d ratio and the radius of cell "a" is 4 times the radius of cell "i." Comparing the pressures at which the sustaining voltage is a minimum for these two cells, we see that the pressure in cell "i" is 4 times larger than that in cell "a." This would seem to indicate that a scaling law exists for the capacitively coupled cells but more "similar" cells must be investigated to be able to say this with certainty.

In either cell "a," "b" or "c," the cells whose thickness is .1 cm, if the pressure is high (above 300 Torr, 240 Torr or 300 Torr respectively) and the 100 KHz sine wave sustaining voltage is applied, the usual light pulses are observed for a number of seconds. Then the cell ceases to refire and remains off for times as long as 60 seconds after which the cell again fires and the process is repeated. If the sustaining voltage is reduced, the frequency of this low frequency "oscillation" is smaller. The "oscillations" occur with no noticeable change in the sustaining voltage. A similar "oscillation" was observed in cell "i," the smallest cell, at pressures below 35 Torr. Francis[20] points out that a dc discharge is sometimes intermittent at low

d	(r/d) for smallest voltage minima (a)	(r/d) for next smallest voltage minima	(r/d) for largest voltage minima
.100	a(.66)	d(.50)	g(.18)
.050	b(1.42)	h(.34)	
.025	f(1.86)	c(3.05)	i(.66)

(a) The letters refer to the curve in Figures 4.2 and the cells in Table 4.1.

Minimum Voltage V vs. r/d

Table 4.2

pressures (in neon at pd values below 4) and the time between discharges can be a number of seconds. He attributes this phenomena to changes of the cathode surface due to gas sorption. It is possible that gas sorption contributes to the "oscillations" in the ac discharge as well.

4.3 Experiments with Gas Mixtures and Molecular Gases

The experimental cell which was used for these experiments had the same dimensions as that used in the experiments discussed in section 4.1 i.e. the thickness is .1 cm and the diameter is .133 cm. When we add small amounts of nitrogen to neon, the light pulses are considerably sharpened. Figure 4.3 shows oscillograms of the light output for different amounts of nitrogen added to 40 Torr of neon. We see that the pulse gets narrower with larger concentrations of nitrogen; the pulse width changes from 2×10^{-6} seconds in neon alone to 3×10^{-7} seconds in neon plus 10% nitrogen. As the pulse width narrows, its amplitude increases and the discharge is more intense.

Other molecular gases in neon also yield sharp pulses. In neon plus 10% water vapor the light pulse width is 3×10^{-7} seconds and in neon plus 10% carbon monoxide the current pulse width is 2×10^{-7} seconds. In Figure 4.4 we show the light pulse for pure neon, neon plus 10% nitrogen, neon plus 10% water vapor and the current pulse for neon plus 10% carbon monoxide.

With nitrogen the discharge is extremely rapid and in Figure 4.5 we show the nitrogen current pulse for different pressures

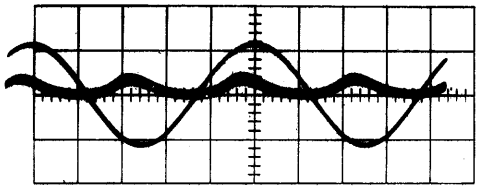

(a) .0 Torr N_2

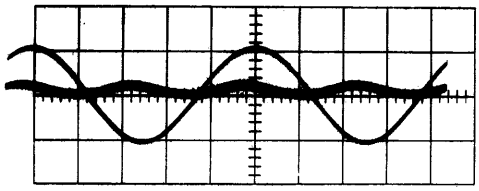

(b) .2 Torr N_2

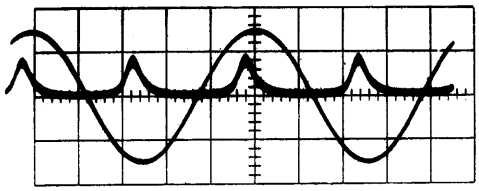

(c) .5 Torr N_2

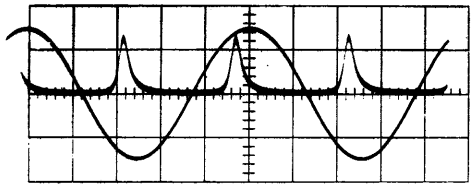

(d) 1.0 Torr N_2

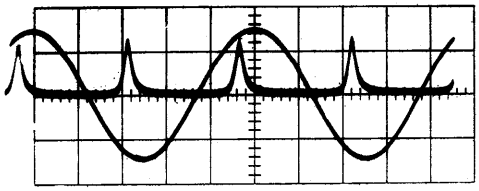

(e) 2.0 Torr N_2

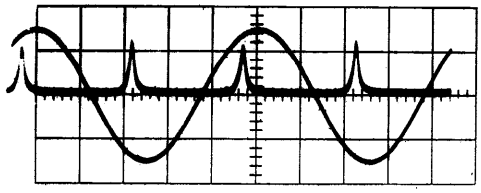

(f) 4.0 Torr N_2

2μs/div

Light Pulse and Voltage
Ne + N_2

Figure 4.3

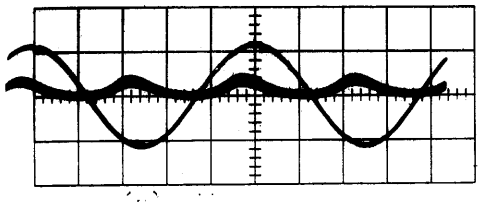

(a) Ne

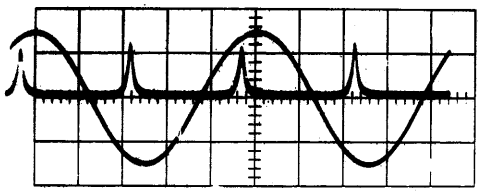

(b) Ne + 10% N_2

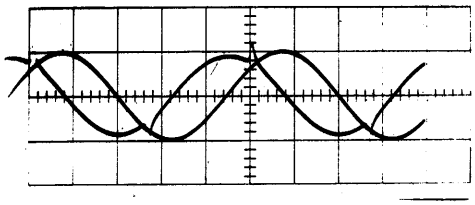

(c) Ne + 10% CO

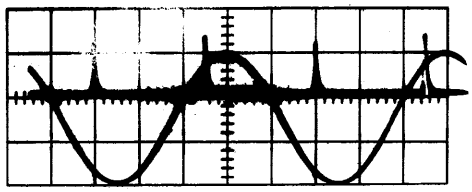

(d) Ne + 10% H_2O

2μs/div

Light Pulses or Current Pulses
for Various Gas Additives

Figure 4.4

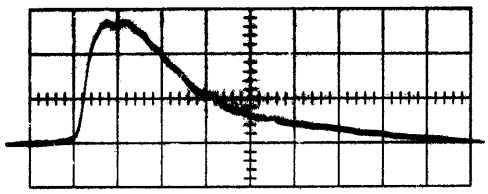

(a) 100 Torr

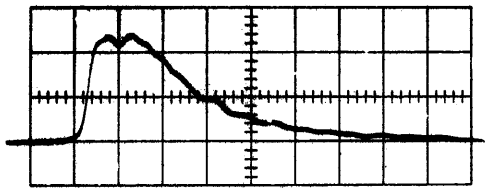

(b) 80 Torr

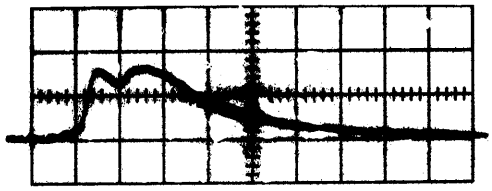

(c) 60 Torr

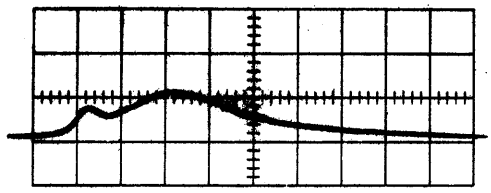

(d) 40 Torr

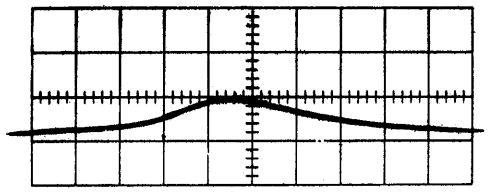

(e) 25 Torr

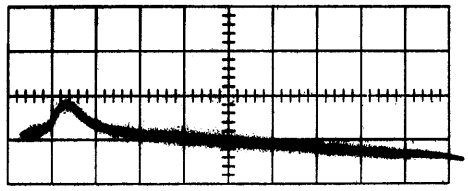

(f) 20 Torr

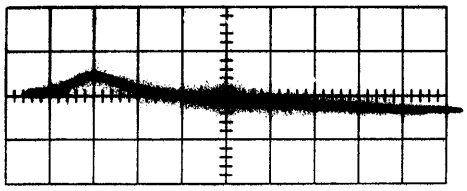

(g) 10 Torr

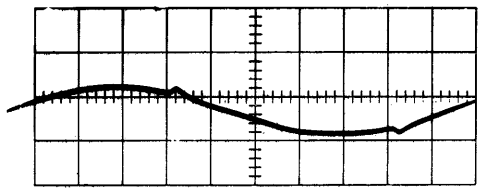

(h) 4 Torr

a-e 10^{-8} sec/div
f,g 10^{-7} sec/div
h 10^{-6} sec/div

Current Pulses in N_2

Figure 4.5

of nitrogen. The current was measured across a small resistor in series with the experimental cell as discussed in Chapter 3. We see that the pulse width decreases as the pressure increases. At pressures above 40 Torr the current pulse has two humps in it indicating that there are two bursts of current. As the ions are practically immobile on this time scale, these bursts must be due to electrons.

We suggest that the sharp pulses that are observed in nitrogen arise from a difference in the secondary electron emission process, which controls the discharge, from that in neon. We believe that, as discussed in Chapter 2, ion bombardment of the cathode is the dominant secondary process in slow neon discharges while in nitrogen, photon bombardment of the cathode is the dominant secondary process. In neon plus a molecular gas, even though the molecular gas concentration is relatively small, we believe that the photon mechanism dominates and increases the speed of the discharge.

The Penning effect increases α in neon-argon mixtures and it seemed worthwhile to determine whether this increase would also yield a rapid discharge. With neon plus 10% argon, the pulse width was 10^{-6} seconds, a value that is larger than the pulse widths in neon plus a molecular gas and this would indicate that an enhanced α does not, in itself, give rapid discharges.

4.4 Separation Between the Firing Voltage and the Sustaining Voltage as a Function of Gas Additive

We would now like to show the firing voltage, V_f', and the sustaining voltage, V_s', as the concentration of gas additive is changed.

Data will be shown for neon plus nitrogen, neon plus carbon monoxide and neon plus argon.

To measure V_f' it was necessary to create a supply of initial electrons. One method of creating these electrons is to illuminate the cell with ultraviolet light. Photoelectrons are emitted from the surfaces and if the amplitude of the sine wave is slowly raised, when V_f' is reached the cell fires. A second method relies on secondary electron emission due to metastable atoms bombarding the surfaces. The sine wave is turned off for 3×10^{-3} seconds every 33×10^{-3} seconds. Metastable atoms have been created in previous discharges. The voltage is raised until the cell fires and is then reduced until the cell ceases to refire. This voltage is taken to be V_f'. We have assumed that the wall voltage, V_o, has decreased to a small value during the off time so that V_f', and not V_s', is observed. We have measured the voltage both ways and the same voltages were obtained so this assumption seems justified. In the following, the second method was used to measure V_f'. Voltage V_s' was measured with a continuous sine wave and V_s' was taken as the voltage at which the cell ceased to refire.

Figure 4.6 shows a graph of V_f' and V_s' as a function of pressure for various gases. In each case, cell "a" (with a thickness = .1 cm and a diameter = .133 cm) is used. This is the same cell that was used in the experiments of sections 4.1 and 4.3. The partial pressure of neon is 40 Torr, and the frequency of the voltage is 100 KHz. We see that at low additive concentrations both V_f' and V_s'

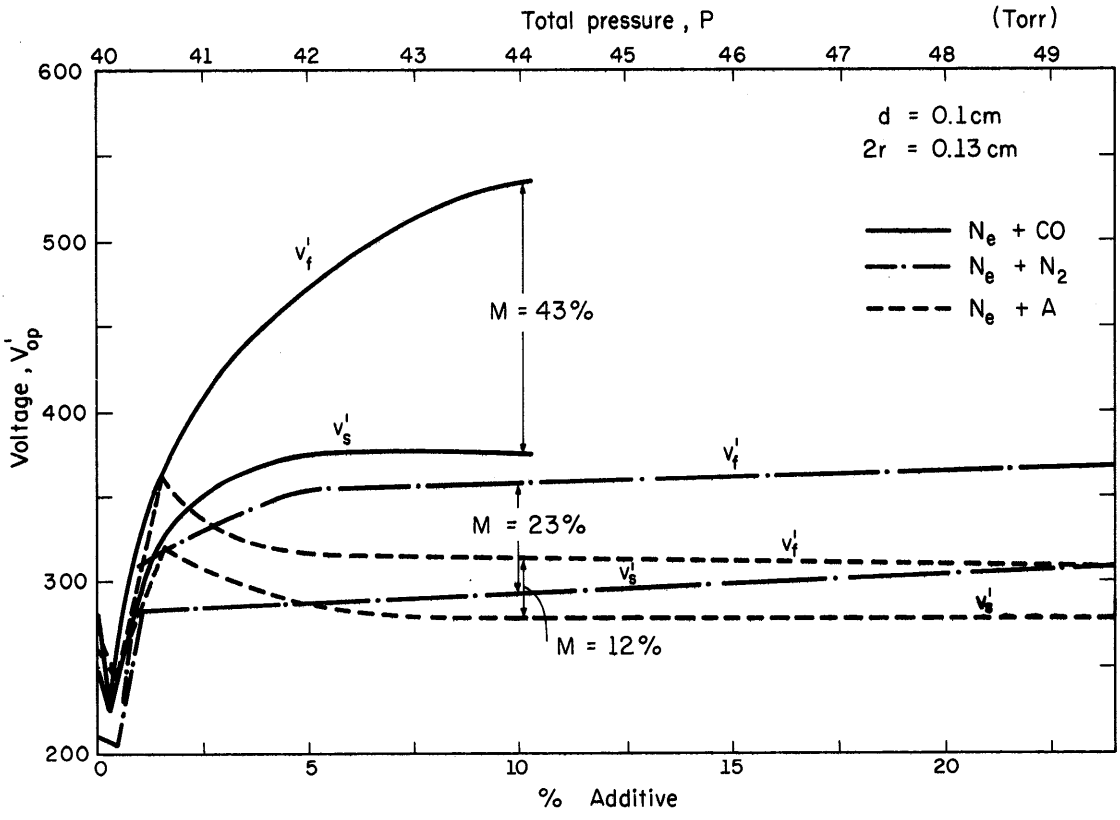

Firing Voltage, V_f', and Sustaining Voltage, V_s'

V_s Gas Additive

Figure 4.6

decrease as the concentration increases until, between .25% to .5% concentration, V_f' and V_s' are equal. With the molecular gases, beyond this point, V_f' and V_s' increase until at higher concentrations the differences between V_f' and V_s' becomes constant. The behavior of the curves for neon plus argon after the minima is somewhat different. Here V_f' and V_s' increase to a maximum separation, and thereafter the two curves decrease to constant values preserving the separation between V_f' and V_s'. With a molecular gas as an additive, at a given percentage concentration, larger voltage separations are obtained than with an inert gas as the additive. Of the two molecular gases, carbon monoxide yields a larger voltage separation than does nitrogen. Unfortunately, the carbon monoxide decomposes in the discharge and deposits carbon on the cell face obscuring the discharge. The figure of merit in neon plus 10% carbon monoxide is 43%, for neon plus 10% nitrogen it is 23%, and for neon plus 10% argon it is 12%. We mentioned in section 4.2 that very little difference was obtained between V_f' and V_s' in neon. The figure of merit was 8% at 40 Torr.

Neon at 300 Torr and nitrogen at 20 Torr was added to cell "i," the smallest cell tested. Extremely narrow pulses were observed. Figure 4.7a shows the current pulse, and we see that it is initiated and turned off in about 25×10^{-9} seconds. The width of the light pulse is 25×10^{-9} seconds. The peak current was 500×10^{-6} amperes, and the charge transferred in this pulse was about $.625 \times 10^{-11}$ coulombs. Neither of the techniques used to measure V_f' for the large cell gave reliable results for the small cell, so the method

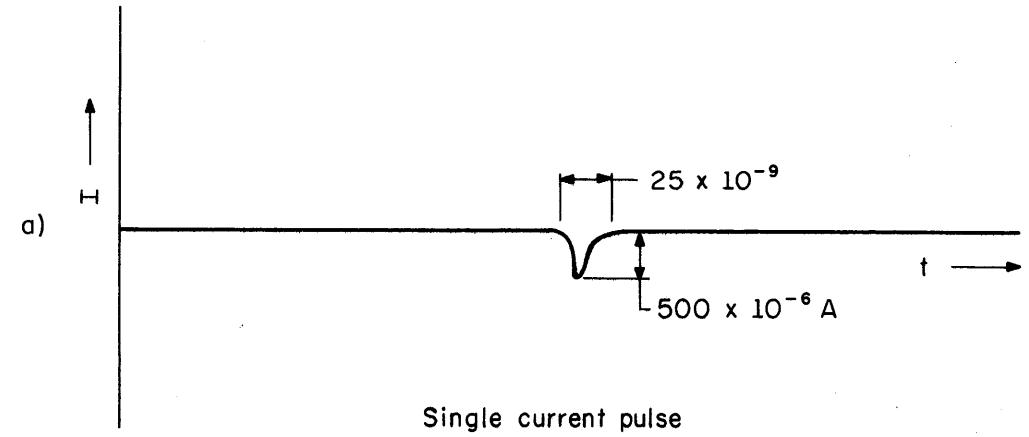

Single current pulse

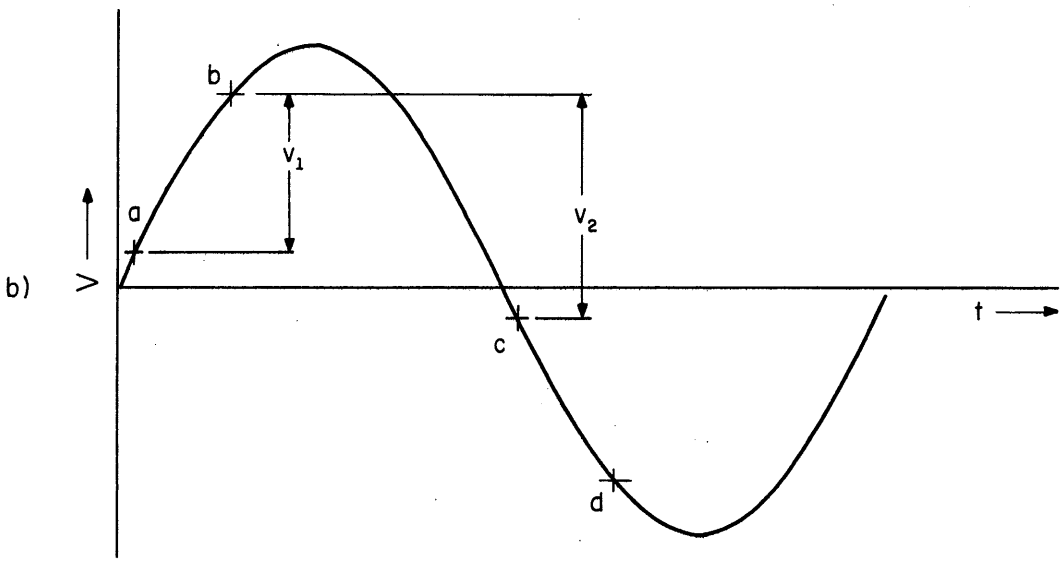

Voltage

Current Pulse and Voltage
for Double Firing

Figure 4.7

described in Chapter 2 where the cell fires twice each half cycle was used to determine the firing voltage and the wall voltage.

At higher voltages, the cell did fire twice each half cycle confirming the predictions made in Chapter 2. The points at which the cell fired are indicated by horizontal lines on the voltage waveform shown in Figure 4.7b. The voltage change between points a and b, V_1, is 600 volts and that between points b and c, V_2, is 750 volts. Using Equations 2.14 and 2.13 we obtain 675 volts for the firing voltage, V_f', and 300 volts for the wall voltage, V_o'. From this, we have that the figure of merit is 80%.

We can estimate the average power to ignite the cell from the product of V_d' at point a, and the observed current blip, in Figure 4.7, averaged over a half cycle. We obtain that the power necessary to excite the cell is of the order of $.844 \times 10^{-3}$ watts.

In Table 4.3 we summarize the pulse width data, τ, and the figure of merit, M, (the memory) for the various gases and gas mixtures for cell "a" (the large cell), and we observed that normally the figure of merit increases as the light pulse width decreases, but if the pressure is too low, small figures of merit are obtained even with narrow pulses. In Figure 4.8 we have plotted this data and we see that $\ln \tau$ is approximately proportional to $\ln M$ and that $M = K_1 \tau^{-K_2}$ where $K_1 = .0019$ and $K_2 = .63$.

Gas	Pressure Torr	Discharge Pulse Width τ $\times 10^6$ sec	Figure of Merit M%
Ne	40	2.0	8%
Ne + 10% A	44	1.0	12%
A	40	0.6	16%
Ne + 10% N_2	44	0.3	23%
Ne + 10% H_2O	44	0.3	24%
Ne + 10% CO	44	0.2	43%
N_2	40	0.06[a]	76%
N_2	4	0.2	8%

(a) Current pulse

Discharge Pulse Width τ and the Figure of Merit for Various Gases for Cell .1 cm Thick and .13 cm in Diameter

Table 4.3

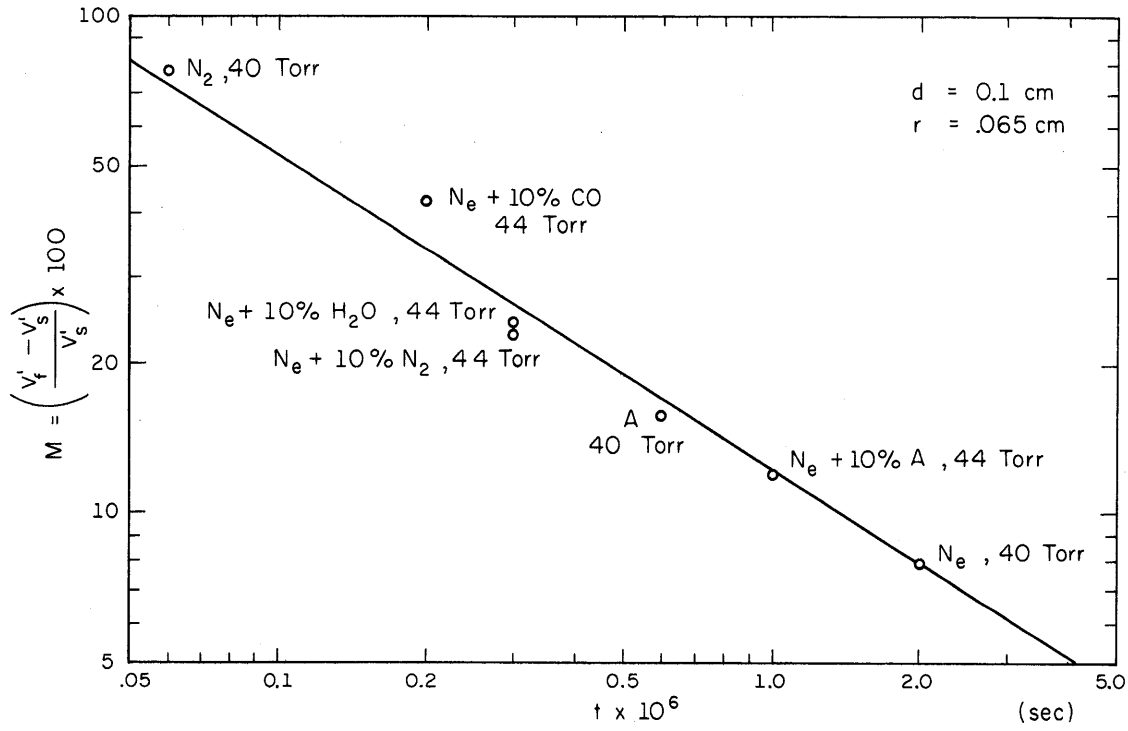

Pulse Width vs. Figure of Merit

Figure 4.8

CHAPTER 5

SWITCHING NETWORKS

A complete matrix has not yet been constructed. However, we have considered techniques for writing cells in an array. Consider a matrix display with n rows and n columns. To address each cell separately requires a switching network sufficiently complex to address n^2 cells. On the other hand, with the physical arrangement shown in Figure 1.1b, this number can be considerably reduced. A single row electrode, and a single column electrode specify the cell common to the two electrodes. A voltage applied to these two electrodes appears across the common cell, but only half of this voltage appears across each of the remaining cells in the row and column, and of course none of the applied voltage appears across the rest of the cells of the array. It is thus possible to address all of the cells in the matrix by specifying only one line in each set of electrodes and only a total of 2n lines need be addressed. The necessary information for doing this is contained in two computer words, each ℓ bits long, where $n = 2^{\ell}$. Any pair of lines can therefore be selected through a pair of switching trees each consisting of ℓ switches.

A simple relay switching tree which will do this is shown in Figure 5.1 for the case where $\ell = 4$. The fanout will be similar for any size ℓ. The binary word of length ℓ selects the row of the matrix in the following manner. The switch nearest the display corresponds to the first bit, the next switch the second bit, etc., where word bits are numbered from right to left. If in the horizontal network the

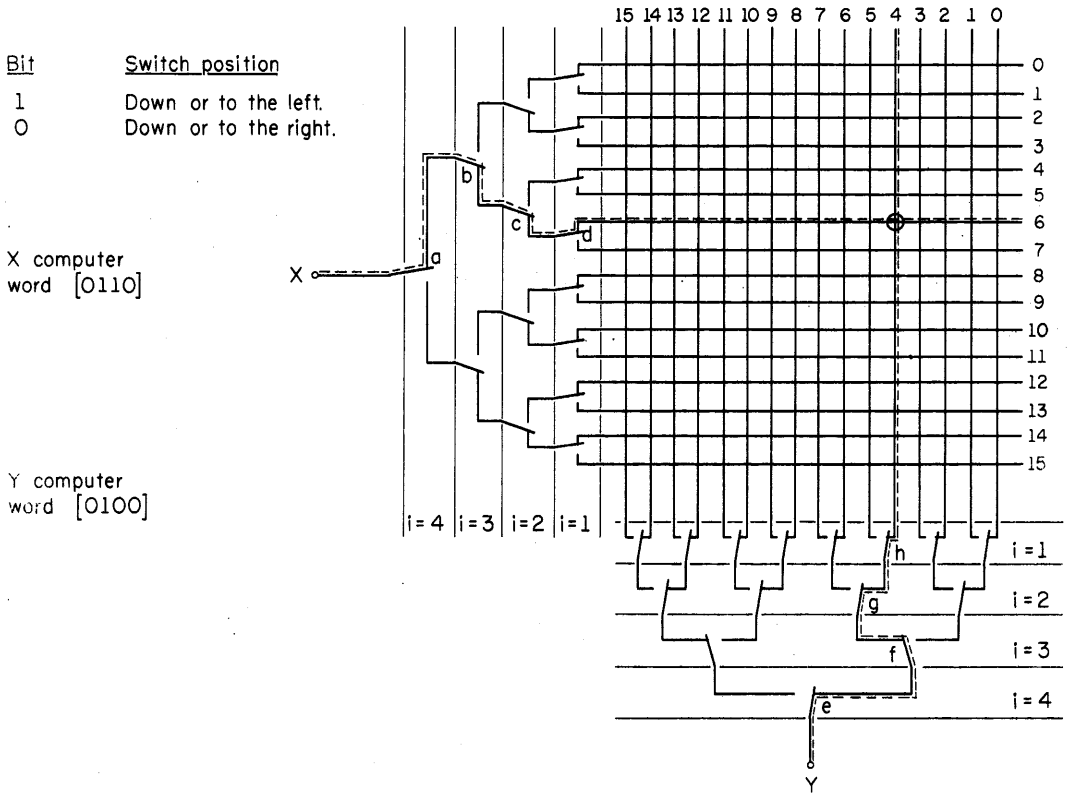

Relay Switching Networks

Figure 5.1

i^{th} bit is 1, the levers of switch i are connected to the lower contacts, but if the bit is 0, the levers are connected to the upper contacts. For example, the computer word for the horizontal switching network is 0110 and path abcd is connected between terminal X and row 6 of the display. Likewise, if the computer word for the vertical switching network is 0100, column 4 is connected by path efgh, to terminal Y. Thus if one applies appropriate voltages to terminals X and Y, the state of the cell common to row 6 and column 11 will be changed.

It seems possible that a more compact and faster switching network can be made from gas cells. These cells would be filled with an appropriate gas so that the cells would remain fired for a large fraction of a half cycle. In addition electrodes would be in the discharge volume permitting direct connection of the branches of the switching tree. Figure 5.2 shows an X and a Y switching network connected to a display consisting of 64 cells. As before, binary words of ℓ bits select paths in the switching networks. Consider the horizontal switching network. The first bit corresponds to the first column of cells on the left of the buffer column, the second bit the second column to the left of the buffer column, etc., where again the word bits are numbered from right to left. Corresponding to the i^{th} bit there are two terminals T_i and $\overline{T}_i$. If the i^{th} bit is 0, signal S is applied to T_i and signal $\overline{S}$ to $\overline{T}_i$; but if it is 1, signal S is applied to $\overline{T}_i$ and signal $\overline{S}$ to T_i. Signal S is also applied to T_r and signal $S + S_s$ to T_b. Signal $\overline{S}$ is the negative of

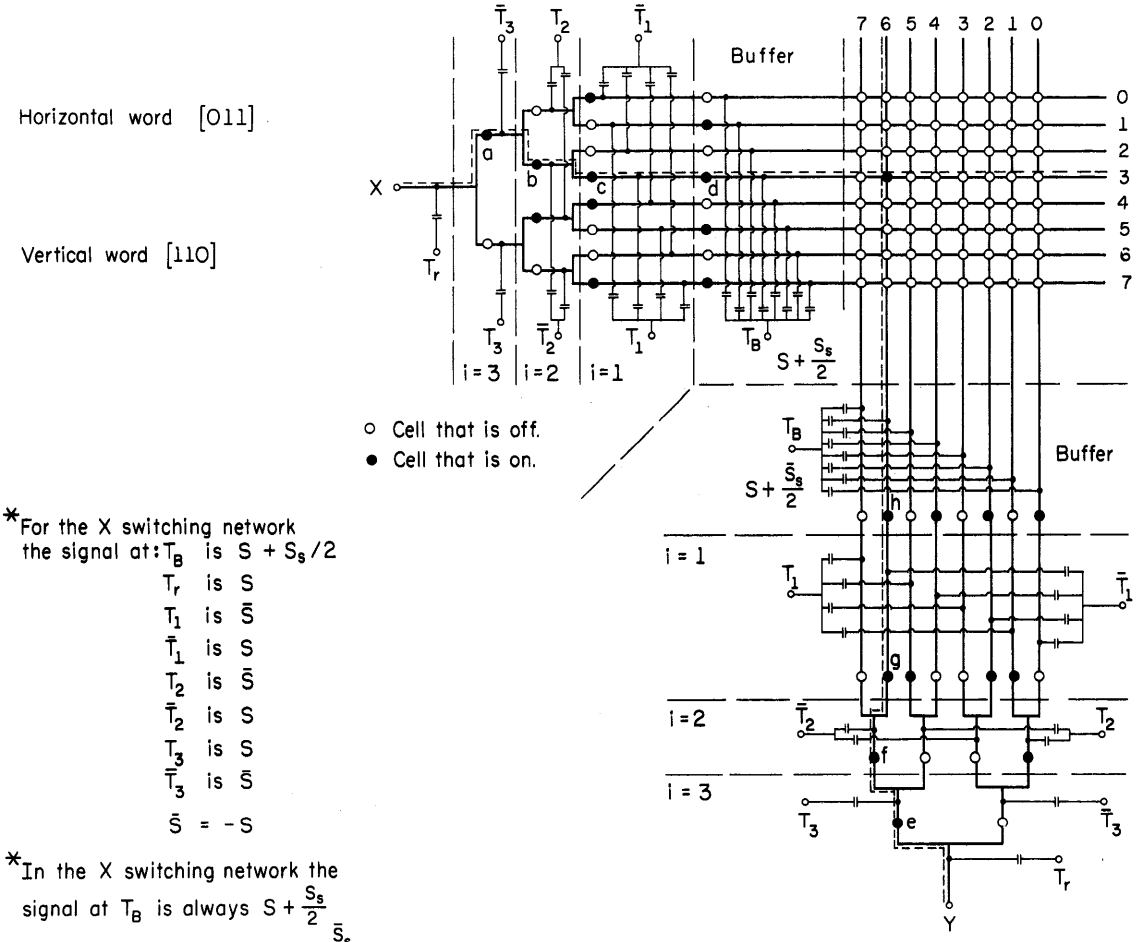

*For the X switching network the signal at: T_B is $S + S_s/2$
T_r is S
T_1 is $\bar{S}$
$\bar{T}_1$ is S
T_2 is $\bar{S}$
$\bar{T}_2$ is S
T_3 is S
$\bar{T}_3$ is $\bar{S}$
$\bar{S} = -S$

*In the X switching network the signal at T_B is always $S + \frac{S_s}{2}$ and in the Y network it is $S + \frac{\bar{S}_s}{2}$.

Gas Cell Switching Networks

Figure 5.2

signal S and only cells with $\overline{S}$ and S across them will fire. In Figure 5.2, word 011 selects path abcd to row 3 of the matrix and word 110 selects path efgh to column 6 of the matrix. During the relatively long time that these cells are fired they have a low impedance and signals applied to terminals X and Y are applied to the common cell in the matrix thereby changing the state of the cell.[8] Notice that there is an impedance, Z_s due to the switching networks in series with each selected row and column of the display. This impedance is equal to $(2\ell + 2)Z_f$ where Z_f is the impedance of a single, fired cell in the switching network. However, as we mentioned in Chapter 2, a conservative estimate gives that the total impedance in series with a display cell can be as large as 10^5 without causing unwanted cells in the array to fire. Therefore for an array of 256×256 cells, $\ell = 8$ and the impedance of a fired, switching network cell, can be as large as $5 \times 10^3 \Omega$ without causing adjacency firing problems.

The display array itself is excited by sustaining signals at the two terminals T_B. At the upper terminal, the signal is $S + \frac{S_s}{2}$ and at the lower terminal, the signal is $S + \frac{\overline{S_s}}{2}$. The actual sustaining signal across all cells in the array is S_s. The buffer stage in each switching network isolates the switching network and the display except at the chosen row and column.

A switching array for $\ell = 3$ has been constructed from neon gas discharge cells (Ne 2's). Appropriate voltages, S and $\overline{S}$, were applied and the array did connect the selected electrode to the input terminal.

CHAPTER 6

SUMMARY

6.1 Summary of Results

We have shown a simple model of the capacitively coupled, gas discharge cell and have used this model to explain the memory mechanism. This model was also used to predict the behavior of the cell with large excitating voltages, and this behavior was subsequently confirmed by experiment. We have also shown that the capacitive reactance should electrically isolate cells from each other when they are interconnected in an array thereby eliminating ambiguities in addressing.

With nitrogen at 40 Torr, probably photon bombardment of the negative surface is the dominant secondary process while in neon at 40 Torr, positive ion bombardment of the negative surface is probably the dominant secondary process. Furthermore, the secondary coefficients which we calculated for these processes are consistent with those given by the literature. It was also suggested that metastable atoms colliding with the cathode probably account for the initial source of electrons which are necessary for reigniting the discharge.

We found that the discharge was turned off once each half cycle, but only in certain gases or gas mixtures are the discharges sufficiently intense and rapid to build up an appreciable wall voltage. We saw that in neon-nitrogen mixtures at increased amounts of nitrogen, the discharge was more abrupt and more intense and that the wall

voltage was larger. Furthermore, we saw that for various gas or gas mixtures the narrower the light pulse, the larger the figure of merit.

Finally, we considered the problem of selecting cells in a matrix and showed a switching network whose switching elements are gas cells with which it should be possible to coincidently select a row and column electrode in an array of cells. By applying appropriate voltages to these electrodes, one can change the state of the cell at the intersection of the two electrodes.

6.2 Suggestions for Further Research

Experiments should be performed to study the characteristics of a small matrix of cells. The extent of the isolation between adjacent cells, the variation in the cell characteristic from cell to cell and the uniformity in the time of ignition should be determined.

Work should be done to develop switching networks made of gas cells. Fabrication of these networks can be similar to that of the display matrix.

If the display matrix proves useful more detailed work should be done on the gas discharge parameters with a view toward optimizing the performance of the cell.

BIBLIOGRAPHY

1. Josephs, J. "A Review of Panel Type Display Devices," Proc. I.R.E., 1380, (1960).

2. Cobine, J. D. Gaseous Conductors, Dover Publication, Inc., N. Y., 1958.

3. Moore, D. W., "Gas Discharge X-Y Display Panel," Winter Convention on Military Electronics, P. G. M. E. of the I. R. E., 8, (1963).

4. National Union Electric Corporation Engineering Bulletin entitled "Lattice Videatron," Orange, N. J., April, 1955.

5. Harris, F. H., Private communication concerning work on matrix displays done by Skellet at the National Union Corporation in November, 1954.

6. Lear, Incorporated, "X-Y Matrix Display," Final report for Contract #N62269-1246, U. S. Naval Air Development Center, Johnsville, Pa., March 1962.

7. Lear Siegler, Inc., Q. P. R., #2, 3, 4, 5, 6, and 7 entitled "Development of Experimental Gas Discharge Display," Contract #Nobsr-89201 Bu Ships, August 1963 through June 1965.

8. Bitzer, D. L., Slottow, H. G., and Willson, R. H., "A Preliminary Description of the C.S.L. Plasma Display," Internal C.S.L. Report, Dec., 1965.

9. Bitzer, D. L., Slottow, H. G., and Willson, R. H., "Gaseous Display and Memory Apparatus," Application for United States Letters Patent #521, 357 dated Jan. 1966.

10. Geppit, Basic Electronic Tubes, McGraw Hill, Inc., N. Y., 1951.

11. von Engel, A., Ionized Gases, Clarendon Press, Oxford, 1966.

12. Francis, G., Ionization Phenomena in Gases, Butterworth Publication, London, 1960.

13. Loeb, L. B., Basic Processes of Gaseous Electronics, University of California Press, Berkeley, 1961.

14. Brown, S. C., Basic Data of Plasma Physics, M.I.T. Press, Cambridge, 1961.

15. Lewin, Fundamentals of Vacuum Science and Technology, McGraw Hill, Inc., N. Y., 1966.

16. Druyvesteyn, M. J., Penning, F. M., "The Mechanism of Electrical Discharges in Gases of Low Pressure," Rev. Mod. Phys., 12, 87 (1940).

17. Dieke, G. H., American Institute of Physics Handbook, McGraw Hill, Inc., N. Y., 1957.

18. Raether, H., Electron Avalanches and Breakdown in Gases, Butterworth, Inc., Washington, D. C., 1964.

19. Meek, J. M. and Graggs, J. D., Electrical Breakdown of Gases, Clarendon Press, Oxford, 1953.

20. Francis, G., Handbuch der Physik, XXII, Springer Verlag, Berlin, 1956.

VITA

Robert Harry Willson was born on November 14, 1936, in Springfield, Illinois. He received the B.S. degree in Engineering Physics from the University of Illinois at Urbana, Illinois in 1959 and he received the M.S. degree in Physics from the same institution in 1961. He transferred to the Department of Electrical Engineering at the same institution in 1961.

He worked for the Sangamo Electric Corporation in Springfield, Illinois the summers of 1954 through 1958 and for Autonetics (A division of North American Aviation, Inc.) in Anaheim, California the summers of 1959 through 1961. He was also a consultant for Autonetics during the fall of 1961. He has been a teaching assistant in Physics, and a research assistant in the Coordinated Science Laboratory.